TPE-FLUOROGENS SHOWING AIEE PHENOMENON FOR SENSING OF Al^{3+} IONS

A dissertation report submitted in partial fulfillment of the requirements for the award of the degree of

Master of Science

in

Chemistry

by

Pranshu

(Reg. No. 301502028)

Under the esteemed guidance of

Dr.Vijay Luxami

Associate Professor, SCBC

School of Chemistry and Biochemistry,

Thapar University, Patiala

July-2017

Dedicated to my
family and
friends

CERTIFICATE

This is to certify that the thesis entitled " **TPE-Fluorogens Showing AIEE Phenomenon For Sensing of Al^{3+} Ions** " submitted by **Mr. Pranshu** in the partial fulfillment of the requirements for the degree of **Master of Science** in **Chemistry** from **Thapar University, Patiala** is a bonafied piece of work carried out under the guidance and supervision of **Dr. Vijay Luxami**, Associate Professor, School of Chemistry and Biochemistry, Thapar University, Patiala and no part of this project has been submitted for the award of any degree in this or any other university.

Pranshu

This is to certify that the above statement made by student concerned is correct and true to the best of my knowledge.

Dr. Vijay Luxami
Associate Professor,
School of Chemistry and Biochemistry,
Thapar University, Patiala.

CANDIDATE'S DECLARATION

I hereby certify that the work which is being presented in the dissertation entitled, **"TPE-Fluorogens Showing AIEE Phenomenon For Sensing of Al^{3+} Ions"** in the partial fulfillment of the requirement for the award for the Degree of Masters of Chemistry, submitted to School of Chemistry and Biochemistry of Thapar University, Patiala, is an authentic record of my own work carried under the supervision of **Dr. Vijay Luxami**. It refers others researcher's work which are duly listed in the reference section. The matter contained in this dissertation has not been submitted, neither in part nor in full to any other degree to any other university or institute except reported in text and references.

Place: PATIALA

Date: 5-9-17

Pranshu

This is to certify that the above statement made by the candidate is correct and true to best of my knowledge.

Date: 5-9-17

Dr. Vijay Luxami
Associate Professor,
School of Chemistry and Biochemistry,
Thapar University, Patiala.

ACKNOWLEDGEMENT

First and foremost, I take the privilege to offer my deepest sense of gratitude to **Dr.Vijay Luxami**, Associate Professor, Thapar University, Patiala, for her commendable support and constant motivation throughout this report. With deep humility, I thank her for all the insightful conversations and his valuable comments. Her guidance has helped me to improve my knowledge and perspective towards the work. I will always be indebted.

I am thankful to **Dr. Kamaldeep Paul**, Associate Professor, Thapar University, Patiala, for constantly encouraging and helping me to put my best in my research project.

My sincerest thanks to **Dr. Amjad Ali**, Associate Professor and Head of Department; **Dr. Bonamali Pal** (former Head of Department), all the faculty members and staff of School of Chemistry and Biochemistry of Thapar University, Patiala, who have best owed their guidance at appropriate time, without which it would have been very difficult to proceed with my work. I would also like to acknowledge Sophisticated Analytical Instruments Laboratories, Patiala; Central University Punjab, Bathinda and Guru Nanak Dev University, Amritsar for providing various research facilities.

I would like to thank my all lab mates especially Gulshan Kumar and Iqubal Singh for helping me throughout my project. Also, I want to thank my all friends especially Nishant Thakur, Aashmeen Kaur, Bharvi Sharma, Sahil Gasso, Riteish Kakas, Neeraj Manwani, Santhosh Reddy, Disha Arora, Renuka and Raveena for always being so supportive and encouraging me with their love and best wishes.

Pranshu

LIST OF ABBREVIATIONS

G	Grams
ml	Milliliters
Mmol	Millimoles
CAN	Acetonitrile
MHz	MegaHertz
m.pt.	Melting point
^{o}C	Degree Celsius
$CDCl_3 - d_1$	Chloroform – d_1
δ	Chemical shift
THF	Tetrahydrofuran
DMSO – d_6	Dimethylsulfoxide – d_6
AIE	Aggregation-Induced Emission
RIR	Restrictions on Intramolecular Rotations
TICT	Twisted Intramolecular Charge Transfer
AIEE	Aggregation-Induced Emission Enhancement
ESIPT	Excited State Intramolecular Proton Transfer
GSIPT	Ground State Intramolecular Proton Transfer
FE-SEM	Field Emission Scanning Electron Microscopy

TABLE OF CONTENTS

ABSTRACT

Tetraphenylethylene based Schiff bases **4** and **5** have been synthesized. Probes **4** and **5** exhibit highly selective absorption and emission behavior towards Al^{3+} ions. Probes display unique AIEE (Aggregation Induced Emission Enhancement) phenomenon in combination of Excited State Intramolecular Proton Transfer (ESIPT) and ion-induced aggregation. The probes in the the presence of Al^{3+} ions showed visible color change from yellow to colorless under visible light and lighten-up emission under UV-light. The probes **4** and **5** showed the lowest detection limit of 0.47 μM and 0.3 μM respectively. The probe **4** upon aggregation showed morphological change from amorphous spheres to crystalline needles whereas probe **5** showed morphological change from spheres to agglomerated clusters.

Keywords. AIEE, Ion-induced aggregation, TPE, ESIPT, Schiff bases, Al^{3+} sensor

Chapter-1
Introduction and Review of Literature

1.1 Introduction

Among the various chemical and physical properties of macromolecules, their ability to sense different moieties has gained exceptional attention in the field of supramolecular chemistry. Depending upon their expression of signal for target probe, they have been classified into; ratiometric, fluorimetric and colorimetric sensors.[1–3] The family of fluorometric sensors is growing at very rapid rate due to their low background noise, convenience, rapidity and sensitivity for analysis. Switch on/off fluorescence based chemo-sensors have widespread applications in environmental monitoring, clinical diagnostics, etc.; not only restricted to the target detection but they can also be used for their imaging within the living cells.[4,5] Fluorescent chemosensors in general show the signal in the presence of analyte via various phenomenon like PET, ESICT, FRET, ESIPT, AIE etc. phenomenon.[6–10] Before previous decade, most of the fluorescent sensors were combined with aggregation caused quenching (ACQ) properties. Recently reported, TPE-based moieties and TPE itself shows an interesting phenomenon of aggregation-induced emission and aggregation-induced emission enhancement that widen the door of their applications. Briefly discussing, when a non-luminescent molecule upon aggregation tends to emit intense fluorescence is regarded as AIE-active probe. Also, there are some luminogens detected that show enhancement in their emission and tend to show aggregation-induced emission enhancement phenomenon. By utilizing the AIE/AIEE effect along with its sensing ability, switch-on fluorescent sensors can be efficiently and effectively designed. A wide range of TPE-based sensors for bioprobes and various chemicals have been reported.

Another interesting phenomenon expressed by some of the TPE-motifs is excited state intramolecular proton transfer (ESIPT). In this process, a tautomer having distinct electronic structure from the native excited state is produced. The four state (E – E* – K – K*) mechanistic process involved ESIPT is demonstrated in **Figure 1,** where E represents enol form and K represent keto-form.[9] Firstly, ESIPT phenomenon was observed in salicylaldehyde by Waller in 1955. The distinct and noticeable properties of ESIPT based fluorophores are dual emission, large stokes shift (~200 nm), ultrafast process and spectral sensitivity to the medium.[11] The great stokes shift attributed to elimination of self-absorption and internal filter effect.

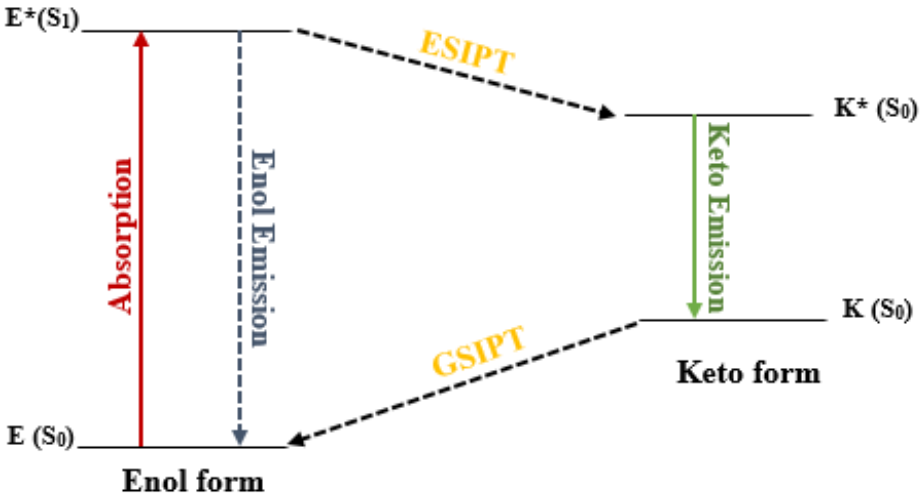

Figure 1. Diagrammatic representation of ESIPT phenomenon.

Basically, this process requires a proton donor site such as -NH_2, -OH, etc. and a proton acceptor site like –C=O, -N=, etc. groups. In a molecule, these donor and acceptor groups should be in close vicinity to each other so that hydrogen transfer becomes feasible. As the enol form of ESIPT based moiety is more stabilized by intra-molecular hydrogen bonding, so, it exists in ground state as enol form. Upon interaction with photons, rearrangement of charges takes place, results in high acidity of donor and the basicity of the proton acceptor. As a result of this increase in polarity, fast proton transfer from donor to acceptor takes place. It leads to tautomeric conversion from the excited state enol form (E*) to excited state keto form (K*) in a very short time period. After decaying radioactively to the ground state, reverse proton transfer occurs to its E form. Different absorbing (E) and emitting (K) molecular species in this intrinsic four-level photo-cycle often leads to total exclusion of self-absorption and the large Stokes' shifted emission. The large stokes shift offered by ESIPT is a useful sensing signal which is required for optical chemo-sensors.

1.2 Literature Review

In last few decades, this unique TPE-family of organic compound possessing AIE (aggregation induced emission) a AIEE (aggregation induced emission enhancement) property has been drastically expanded because of unique features that compounds have displayed, not only in the field of OLEDs (organic light emitting diodes) but also due to their high efficiency in sensors for biological and chemical analysis.[12–16] Tetraphenylethylene based derivatives were used for ion-sensing, biological material recognition, explosive detection, etc.

Tong *et al.* (2006) reported TPE-derivatives **1a-1d** for the turn-on fluorescence detection of bovine serum albumin due to the restrictions on intra-molecular rotations of the dyes in the complexes and aggregates.[17]

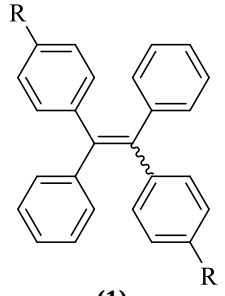

(1)

R = $-O(CH_2)_2Br$ **1a**
$-O(CH_2)_4Br$ **1b**
$-O(CH_2)_2N^+(C_2H_5)_3Br^-$ **1c**
$-O(CH_2)_4N^+(C_2H_5)_3Br^-$ **1d**

Liu *et al.* (2008) designed two tetraphenylethylene (TPE) based turn-on chemosensors **2** and **3** bearing thymine and adenine probes, respectively, for $Hg^{2+}$and Ag^+ ions by taking the advantage of the AIE property of TPE moiety and the specific binding of thymine/adenine with Hg^{2+}/Ag^+.[18]

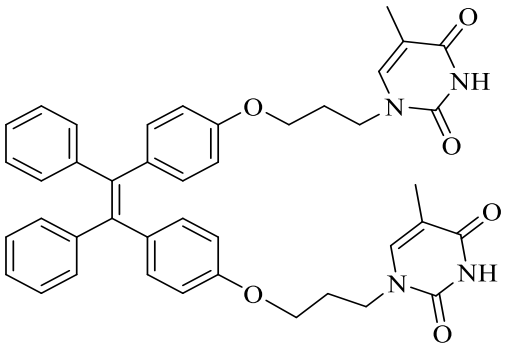

(2)

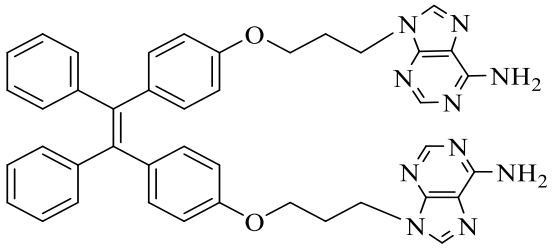

(3)

Chen *et al*. (2010), grafted glucosamine hydrochloride molecules to TPE motif and resulted in a novel cationic water-soluble TPE-derivative **4**. Upon aggregation, the triggered emission properties of compound **4** were used for fluorometric detection to alkaline phosphatase (ALP) via enzyme-induced de-aggregation of the ensemble of **4** and substrate.[19]

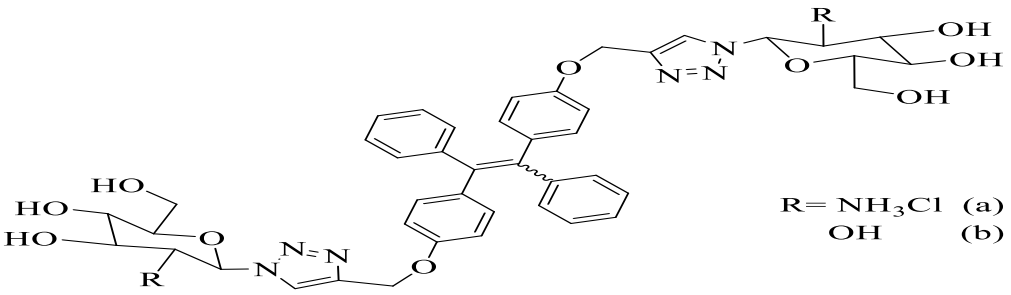

(4)

Park *et al.* (2010) discovered highly efficient 'turn-on' fluorescence ion sensor **5** for the detection of pyrophosphate ions. This TPE-Zn^{2+} based emission sensor showed increase in fluorescence intensity upon binding with PPi in 1:2 (Ligand: PPi) binding ratio.[20]

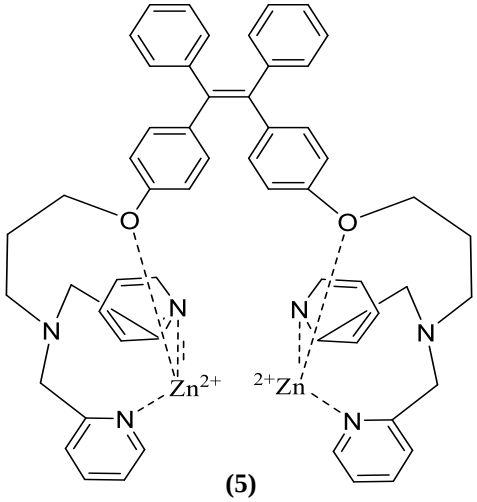

(5)

Hong et al. (2011) synthesized terpyridine-containing tetraphenylethenes **6** and investigated their optical and metal sensing properties. Being a TPE-derivative, upon aggregation their non-luminescent property was transformed to highly emissive nature. A red shift in the emission spectra was observed in the presence of Zn^{2+} ions. Due to the metal- ligand charge transfer process, terpyridine substituted TPEs express a magenta color upon binding with Fe^{2+} ion, allowing the rapid recognition of Fe^{2+} ions in the water media.[21]

Sun *et al.* (2011) was efficiently designed a tetraphenylethylene based highly selective and sensitive probe **(7)** for zinc metal ion detection. This aggregation induced emission based molecule can act as fluorescence turn-on sensor. [22]

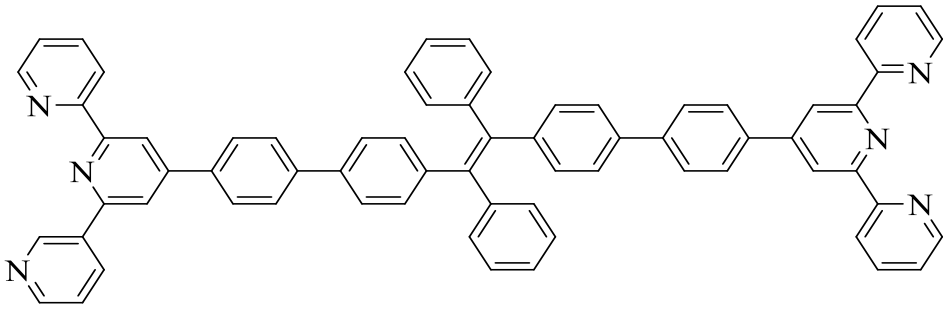

(6)

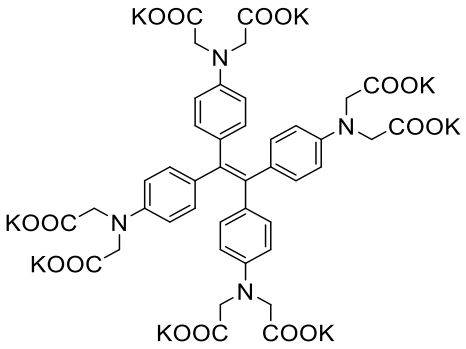

(7)

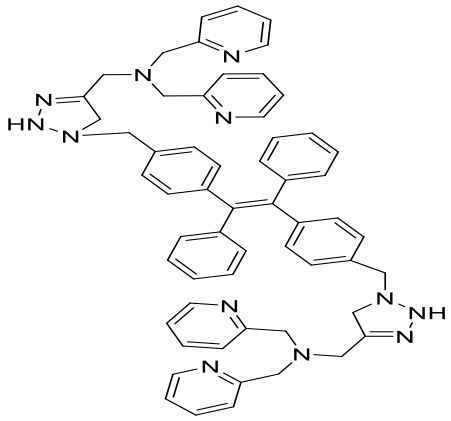

(8)

Ye *et al.* (2012) made the use of click reaction to synthesize tetraphenylethylene-based highly sensitive and ratiometric sensor **(8)** for Ag^{+} ion detection. Sensor exhibit the AIE phenomenon and binds specifically with silver ions in 1:2 (ligand:Ag^{+}) along with expressing enhancement in emission properties.[23]

Ye *et al.* (2012) efficiently synthesized a novel tetraphenylethylene based sensor **9** bearing BODIPY unit and bis(2-pyridin-2-ylmethyl) amine (BPA) unit linked with triazole moieties by click reaction. It formed stable stoichiometric complexes with Cu^{2+} and Co^{2+} in 1:1.[24]

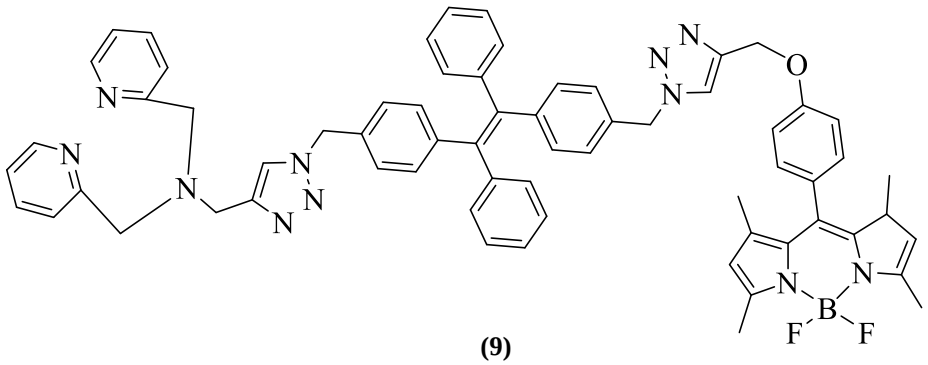

(9)

Zhang *et al*. (2012), designed a new probe **10** exhibiting selective turn-on fluorescence for CN^{-} ions by taking the benefit of aggregation induced-emission (AIE) behavior of tetraphenylethylene blocks and the nucleophilic attack of CN^{-} ion on the indolium group.[25]

Yan *et al.* (2013) designed sensitive and selective fluorescence 'on-off-on' probe **11** based on tetraphenylethylene (TPE) moiety for sequential recognition of Hg^{2+} and Fe^{3+} in water. Importantly, the complex **11**-Fe^{3+}could behave as a 'turn on' fluorescent sensor. The selectivity of this complex for Hg^{2+} ions over other heavy and transition metal ions was appreciable, and its sensitivity for Hg^{2+} ion was 2 ppb in aqueous medium.[26]

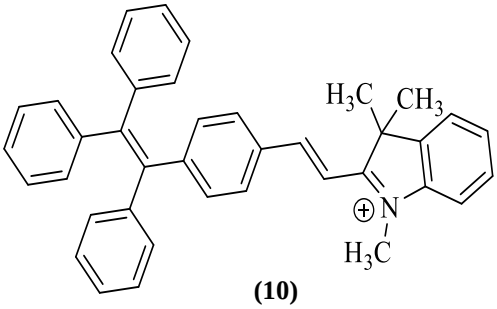

(10)

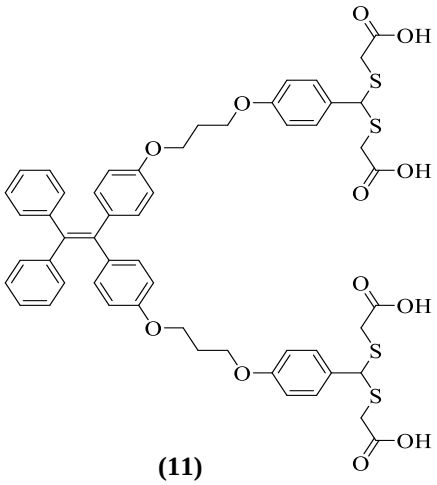

(11)

Feng *et al.* (2013) synthesized chiral TPE-based macrocycles (**12** and **13**) having optical pure amine groups and possess a differentiating ability between the two enantiomers of α-amino acids and chiral acid groups by enantioselective aggregation and aggregation-induced emission effect.[27]

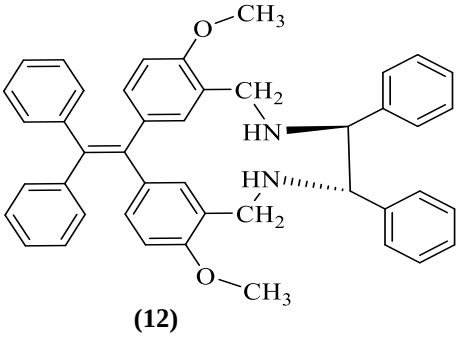

(12)

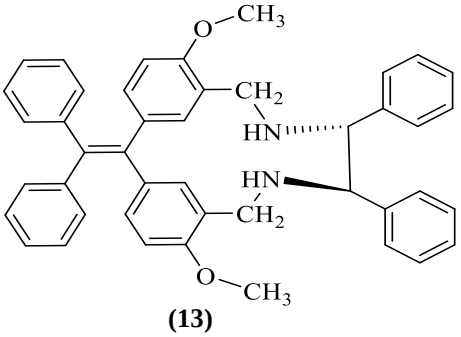

(13)

Gu *et al.* (2013) developed a novel turn-on fluorescence assay for ALP (alkaline phosphates) with TPE-based derivative **14**. This compound was successfully applied for ALP assay in living cells. Moreover, it can be used for screening of inhibitors of ALP.[28]

Turan *et al*. (2013) synthesized a siloxy-functionalized tetraphenylethylene derivative **15** worked an excellent sensor for fluoride ions. The mechanistic behavior is highly selective for fluoride anions and charge transfer resulted in a green colored solution.[29]

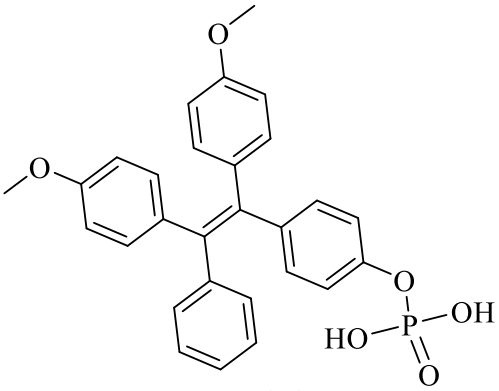

(14)

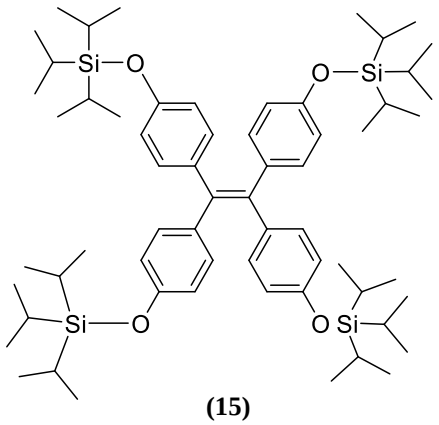

(15)

Ye *et al*. (2014) developed a new TPE-based sensor bearing double 2-ethylpyridyl-2-methylthiophenylamino blocks linked with triazole molecules. Selectivity of **16** towards Fe^{3+} ion over other metal ions was determined by UV-Visible and fluorescence studies. The lowest detection limit of for Fe^{3+} ion was 0.7 μM. 1:2 stoichiometry of **16**-Fe^{3+} complex was confirmed by ^{1}H-NMR titrations.[5]

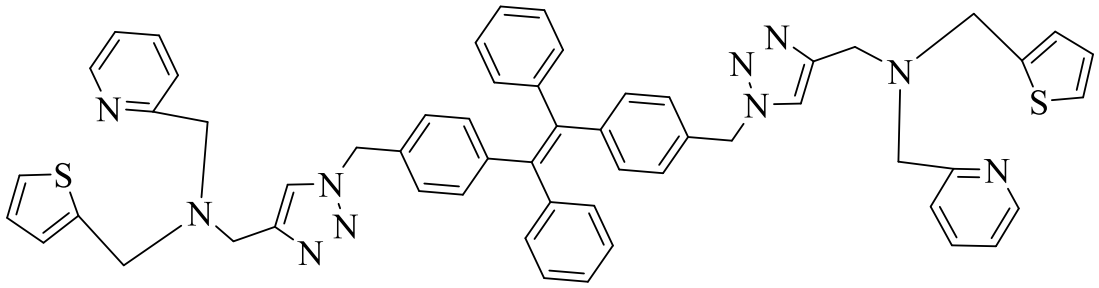

(16)

Feng *et al.* (2014) discussed TPE-based schiff base macrocycle **(17)** expressing an AIE-effect and showing a sensitive response to DNP and TNP among a large number of aromatic compounds. It could detect DNP and TNP to nM levels. Also, this macrocycle could aggregate into nanospheres and emit yellow colored fluorescence in aqueous media. For practical application, it`s sensitivity was checked in real water samples. In the same year, he synthesized another TPE-based macrocyclic moiety **(18)** showing similar kind of properties. Probe **18** was synthesized by the condensation of TPE-dialdehyde and 1,2-benzenediamine. Unlike previous molecule, it was aggregated into nanofibers. This probe was highly sensitive towards copper ions in water medium.[30]

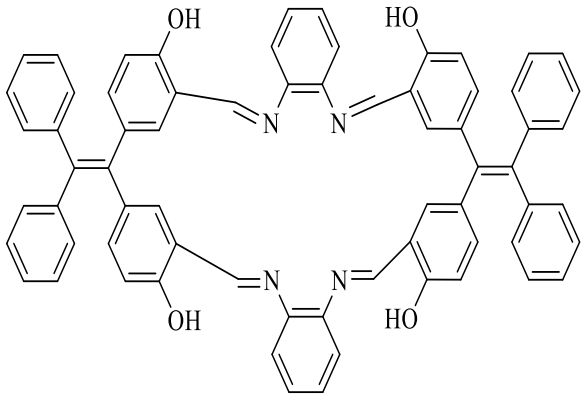

(17)

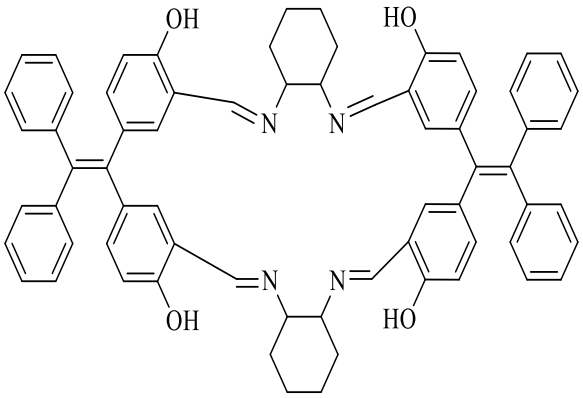

(18)

Gui *et al.* (2015) efficiently construct a TPE based carboxy acid probe **(19)**. As carboxylic acids are readily soluble in water, thus, attachment of carboxy acid group to tetraphenylethylene moiety provides better solublitity in biological systems. This advantage pushes the sensor for better use in aluminium ion detection in living systems. The sensor detection limit was very less (upto nM level). In addition to all these benefits, the AIE effect enables large signal/noise ratio for bio-imaging without washing steps.[31]

Khandare *et al.* (2015), created a sensitive fluorimetric assay for dissolved carbon dioxide (dCO_2) by using ion-induced self-assembly of a TPE-derivative **21** along with taking the advantage of its aggregation induced emission property. Chitosan, a commercially available polymer having amine functionality was utilized for the ion induced assay. The aggregation caused intense blue fluorescence output from the system. A detection limit of 5×10^{-6} M (0.00127 hPa) was obtained. This was the first report for detection of dCO_2 utilizing the AIE property.[32]

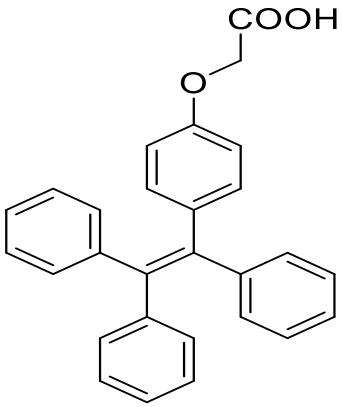

(19)

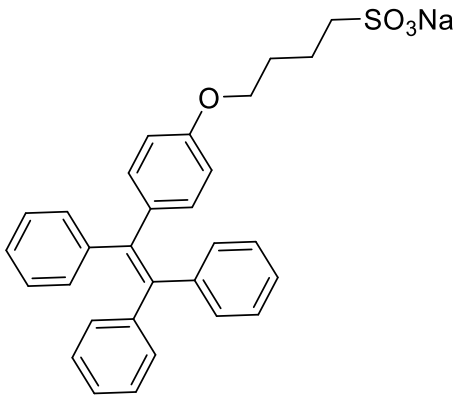

(20)

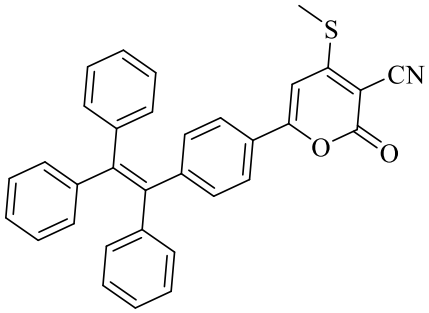

(21)

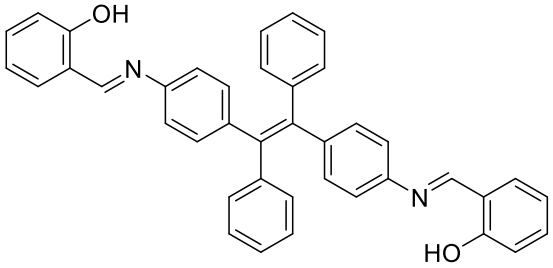

(22)

Mahendran *et al.* (2016) designed tetraphenylethylene-2-pyrone conjugate **(21)** exhibiting donor-acceptor relationship. The fluorescent nano-aggregates were exposed for selective detection of nitro aromatic compounds. Efficient TPEP-based cheap fluorescent strips were developed for the selective detection of picric acid.[33]

Gupta *et al.* (2017) reported a TPE-based schiff base **(22)** exhibiting features of both excited-state intramolecular proton transfer (ESIPT) and aggregation induced emission (AIE). The collective behavior of both AIE and ESIPT showed large stokes shift and high sensitivity towards the detected ions (Cu^{2+} and F^{-}).[34]

1.3 Research Gap

From our literature review, we analyzed that not much work was explored on the Schiff base motifs based on tetraphenylethylene base molecule. A very few TPE-based Schiff bases were reported that exhibit the combined feature of AIE and ESIPT characteristics. Especially, for the construction TPE sensors only single or double position is occupied. According to best of our knowledge there no report on TPE sensor where all the four phenylene moieties are substituted with the receptor site. So, this consideration increases our anxiety to explore aggregation effect on luminogenic TPE-based Schiff bases.

1.3 Objectives

Our aim in this dissertation was mainly concerned with aggregation and sensing properties of tetraphenylethylene based derivatives with the following considerations:

- Synthesis of TPE based chemosensor occupying the all the four phenylene moieties with receptor sites.
- To explore the AIEE phenonomenon of the synthesized molecules.
- To evaluate the chemosensing properties of the synthesized molecules towards various metal ions.

The overview of synthesized molecules are as below:

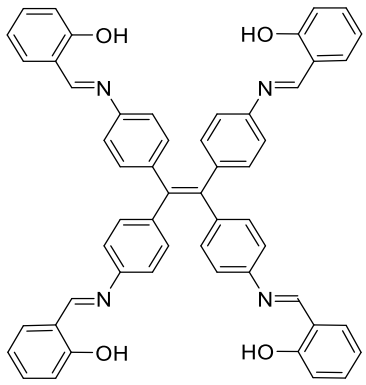

4

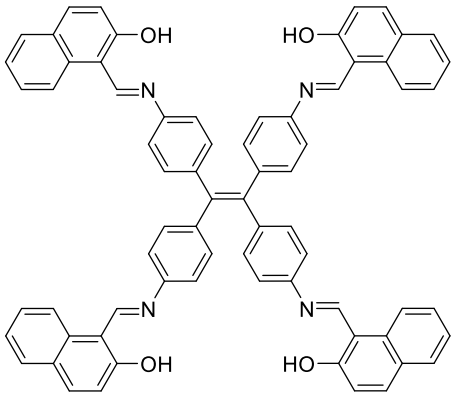

5

Chapter-2
Materials and Methodology

2.1 Materials

Bezophenone (99.0%, Spectrochem), titanium tetrachloride(99.0%, Spectrchem), zinc powder(90.0%, SDFCL), salicylaldehyde(98.0%, Spectrochem), nitric acid (98.0%, Avantor), 2-hydroxy-1-naphthaldehyde(98.0%, Sigma-Aldrich), specially dried tetrahydrofuran(99.5%, Lobal Chemie), carbinol (99.9%, Spectrochem), acetonitrile(99.9%, Spectrochem), sulphuric acid(98.0%, Avantor), chloroform-d_1 (99.8%, MagniSolv) and dimethylsufoxide-d_6 (99.8%, Euriso-top) were used as purchased. All solvents were dried according to the suitable methods before use.

2.2 Methodology

2.2.1 Methodology adopted for synthesis.

Synthetic route for construction of probe **4** and **5** is discussed in next section. Each intermediate product involved was characterized by NMR technique and High Resolution Mass Spectroscopy. ^{1}H and ^{13}C NMR-spectra associated with compounds **2-5** were recorded using chloroform-d_1 and dimethylsulfoxide-d_6 as solvent on JEOL ECS–400 MHz spectrometer using TMS as an internal reference. Chemical shifts were reported in ppm and coupling constants (*J*) were measured in Hz. Multiplicities are abbreviated as s, d, t and m for singlet, doublet, triplet and multiplet respectively. Mass analysis of probe **4** and **5** was performed on BRUKER DALTONIK micrOTOF-Q11 spectrometer using high resolution mass spectroscopy technique.

2.2.2 Methodology adopted for photo-physical studies

In order to determine their photo-physical properties 1×10^{-3} M stock solutions of **4** and **5** using appropriate ratios of acetonitrile and dimethylsulfoxide were prepared. UV-Visible and fluorescence studies with cations (Zn^{2+}, Al^{3+}, Mg^{2+}, K^{+}, Ca^{2+}, Hg^{2+}, Ag^{+}, Pb^{2+}, Co^{2+}, Cu^{2+}, Ni^{2+}, Fe^{2+}, H^{+}, etc.) and anions (Cl^{-}, Br^{-}, F^{-}, CN^{-}, $H_2SO_4^{2-}$, HSO_4^{-}, $H_3PO_3^{-}$,$H_3PO_4^{2-}$, OH, etc.) were performed in methanol to understand the ion sensing behavior of probe **4** and **5**. UV-Visible studies were performed on Shimadzu-2600 spectrophotometer using a quartz glass cuvette of path length 1cm whereas fluorescence analysis was performed on Varian Cary Eclipse fluorescence spectrophotometer. In order to determine the practical applicability of **4** and **5**, UV-Visible and fluorescence spectra of detected ion in presence of other ions were recorded.

Again, absorption and emission studies of **4** and **5** in the presence of ratio-metric quantities of detected ion were performed to determine the stoichiometry of **4** and **5**. Perchlorate salt of detected ion (Al^{3+}) ion was used for absorption and emission titrations. All UV-visible and fluorescence scans were saved in ACS II format and further converted to Excel files to plot various graphs. Binding constant was determined according to the Benesi-Hildebrand equation. K_a was calculated by equation stated below,

$$1/(A-A_o) = 1/[K_a(A_{max}-A_o)\,[M^{x+}]^{n}] + 1/[A_{max}-A_o]$$

where,

A_o= Absorbance of host in the absence of guest,

A= Absorbance of host recorded in the presence of added guest,

A_{max}= Absorbance in the presence of added $[M^{x+}]_{max}$,

K_a= Binding/association constant.

These molecules show an interesting behavior of ion-induced aggregation. In order to study ion-induced aggregation property, FE-SEM studies was performed on ZIESS MERLIN Compact Field Emission- Scanning Electron Microscope.

Root molecule of probe **4** and **5** is tetraphenylethylene moiety. TPE-based derivatives are well known for their unique aggregation based emission responses. So, to study these responses UV-Visible and fluorescence studies, FE-SEM analysis have been performed.

Chapter-3
Experimental Section

3.1 Target molecules construction

Synthesis of probe 1. Probe 1 was synthesized as reported in literature.[22] Under nitrogen atmosphere, a three-necked 250 ml round bottom flask was charged with anhydrous zinc powder (~ 2.4 g, 36.50 mmol) and specially dried THF (100 ml). The suspension was then cooled to 0 ^{o}C, and $TiCl_4$ (~ 2 ml, 10.28 mmol) was added drop wise with syringe by maintaining the temperature below 5 ^{o}C. The chilling reaction mixture was brought to room temperature and stirred for 15-20 minutes and then heated to reflux at 110-120 ^{o}C. After 3 h, the mixture was brought to 80 ^{o}C and solution of benzophenone (1.3 g, 7.17 mmol) in 50 ml THF was added to reaction mixture slowly. Immediately after addition, the reaction mixture was again refluxed at 120 ^{o}C until the reactant was completely consumed (examined by TLC). The reaction was cooled to room temperature and then aqueous solution of 10% K_2CO_3 was added till the pH of mixture gets neutral. Then, the product was extracted using ethyl acetate and water by separating funnel method, from which organic layer was collected and distilled off. Pure cream colored probe **1** (2 g, 84.50% yield) was obtained.

Synthesis of probe 2. The compound **2** was synthesized according to procedure reported in literature.[22] To the solution of probe **1** (1.6 g, 5 mmol) in 25 ml DCM, the mixture of nitric acid (4.2 ml, 10 mmol) and sulfuric acid (6.4 ml, 10 mmol) was dropped added slowly at 0 ^{o}C. The resulting mixture was stirred at 0 ^{o}C for 30 minutes and then the ice bath was removed. The mixture was stirred at room temperature for 6 h until **1** was completely disappeared (monitored by TLC) and then reaction was quenched by pouring ice-cold water in it. Now, the compound was extracted using dichloromethane and water by separating funnel method. The organic layer was collected and distilled off to obtain crude solid. Crude product was purified by silica gel column chromatography using hexane/ethyl acetate as eluent. Bright yellow colored of probe **2** was obtained (1.81 g, 72.20% yield).

Synthesis of probe 3. To the suspension mixture of **2** (0.48 g, 1 mmol) in 100 ml of carbinol, a pinch of palladium-carbon was added. The reaction mixture was allowed to stir at room temperature in the presence of hydrogen gas. Within one hour, the yellow colored suspended mixture was changed to extremely dark red colored solution. After two hours the reaction mixture was filtered over celite layer. The resulting liquid part was distilled off to get dark red colored crude was obtained. This crude was then purified through basified silica gel column chromatography using chloroform/methanol as eluent. Bright red colored solid **3** wasobtained

with 50% yield (0.18 g). ^{1}H NMR (400 MHz, DMSO-d_6):δ (ppm) 6.53 (d, J = 8.0 Hz, 8H), 6.22 (d, J = 8.0 Hz, 8H), 4.82 (s, 8H). This data matches with the data given in literature[22] and confirmed the formation of probe **3**.

Synthesis of probe 4. Solution of compound **3** (0.04 g, 0.25 mmol in 5 ml THF) was prepared and mixed with solution of salicylaldehyde (0.1 g, 1 mmol in 5 ml THF) in 50ml round bottom flask, and mixture was refluxed for about 2 h. After the completion of reaction (monitored by TLC), THF was distilled off and pure solid **4** was obtained.

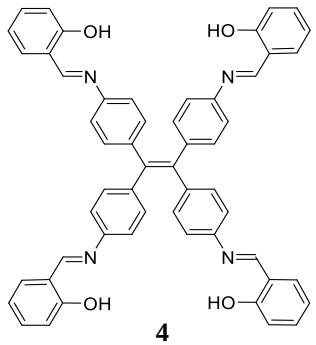

4

Light yellow solid, yield= 90% (0.09 g), m.pt.: 227 ^{o}C, ^{1}H NMR (400 MHz, $CDCl_3$, 400 MHz): δ (ppm) 11.02 (s, 4H, OH), 8.61 (s, 4H, CH), 7.37 (t, 8H, J = 8.0 Hz, ArH), 7.15(q, 16H, J = 8.0 Hz, ArH), 7.00(d, 4H, J = 8.0 Hz, ArH), 6.93(t, 4H, J = 8.0 Hz, ArH). ^{13}C NMR ($CDCl_3$, 100 MHz): δ (ppm) 162.34 (-C-OH), 161.2 (-C=N), 148.8 (ArC), 142.3 (ArC), 140.3 (C=C), 133.2 (ArC), 132.6 (ArC), 132.3 (ArC), 120.9 (ArC), 119.2 (ArC). 119.1 (ArC), 117.3 (ArC). HR-MS (EI) m/z (+Na^+): calculated: 831.3654 (M^+ + Na^+), found: 831.3652 (M^+ + Na^+).

Synthesis of probe 5. To the solution of compound **3** (0.02 g, 0.125 mmol in 5 ml THF), the solution of 2-hydroxy-1-napthaldehyde (0.08 g, 0.5 mmol in 5 ml THF) was added in 25ml round bottom flask, and mixture was refluxed for about 2 h. After the completion of reaction (monitored by TLC), the THF was distilled off.

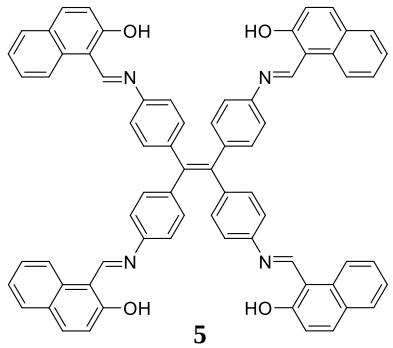

5

Bright orange colored solid, yield= 91.2% (0.05 g), m.pt.: 263 ^{o}C, ^{1}H NMR (400 MHz, $CDCl_3$): δ (ppm) 10.81 (s, OH), 9.92 (s, 4H, CH), 7.99 (d, 4H, J = 8.0 Hz, ArH), 7.78 (d, 4H, J =12.0 Hz, ArH), 7.68 (d, 4H, J = 4.0 Hz, ArH), 7.63 (t, 4H, J = 8.0 Hz, ArH), 7.49 (q, 8H, J = 8.0 Hz, 16.0 Hz, ArH), 7.21 (s, 16H, ArH). ^{13}C NMR ($CDCl_3$, 100 MHz): δ (ppm) 163.7 (-C-OH), 162.8 (-C=N), 154.3 (ArC), 142.3 (ArC), 140.3 (C=C), 139.2 (ArC), 131.2 (ArC), 130.3(ArC), 128.9 (ArC), 127.8 (ArC), 125.1 (ArC), 124.6 (ArC), 123.3 (ArC), 113.5 (ArC). HR-MS m/z (+Na^+): calculated: 1031.3573 (M+ Na^+), found: 1031.3785 (M+ Na^+).

Chapter-4
Results and Discussions

4.1 Synthetic route

Synthesis of Compound 3. Final route for construction of target moieties **4** and **5** is illustrated in scheme **1-3**. Commercially available benzophenone was used to synthesize the molecule **1** by Mcmurry coupling reaction using Zn-$TiCl_4$ system. The root molecule was obtained in very good yield. Compound**1**was treated at 0 ^oC with nitric acid-sulfuric acid mixture 7 h to obtain a bright yellow colored tetra-p-nitro substituted product **2** in 72.2% yield.

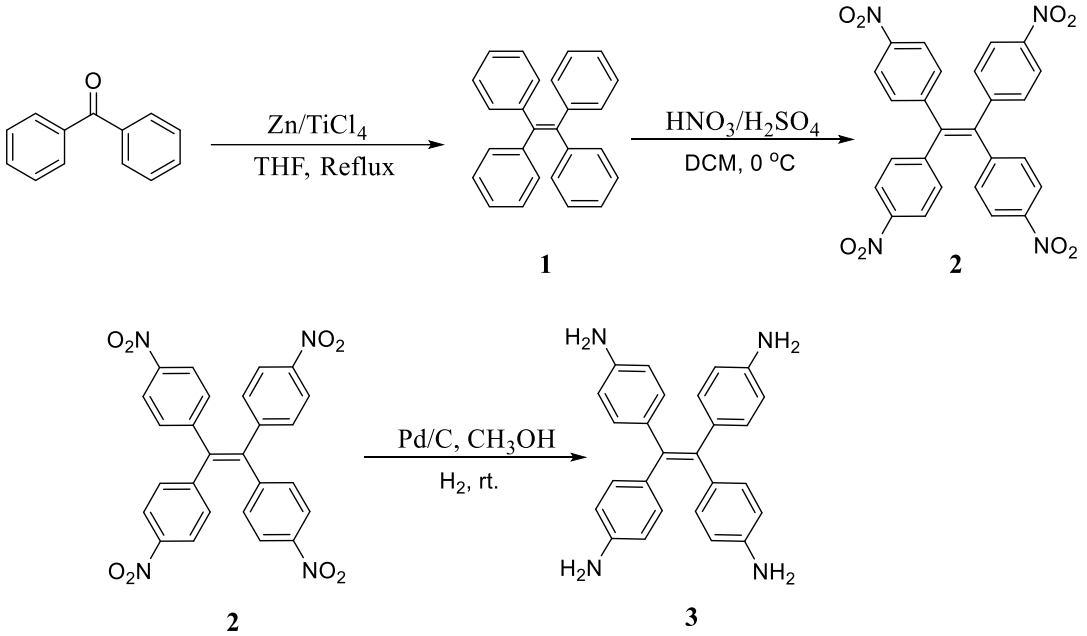

Scheme 1. Synthetic route for compound **3**

Solid of compound **2** was reduced using palladium-carbon as a catalyst in the presence of hydrogen gas. Red colored reduced product **3** was obtained in 50% yield. Probes **2** and **3** were purified by using silica gel column chromatography. ^1H NMR spectrum of probe **3** showed 8H broad singlet at δ 4.28 ppm due to NH_2 protons and two 8H doublets at δ 6.22 ppm and δ 6.53 ppm for aromatic protons. The observed ^1H-NMR spectrum was in accordance to reported spectra of the **3** and confirmed its formation.

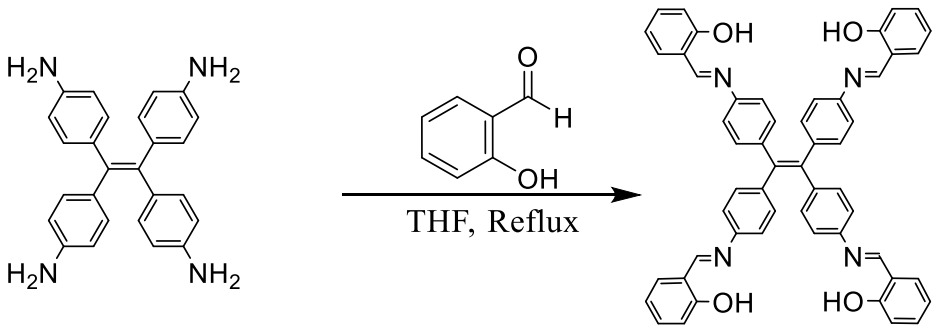

3 **4**

Scheme 2. Synthetic route for probe **4**

Synthesis of Probe 4. Probe **4** was synthesized by refluxing the mixture of probe **3** (0.04 g, 0.25 mmol) and salicylaldehyde (0.1 g, 1 mmol) in THF for 5 h. After completion of refluxing time period, THF was distilled off and light yellow colored solid was obtained in 90% yield. ^{1}H NMR spectrum showed 4H broad singlet at δ 11.02 ppm due to OH, 4H sharp singlet at δ 8.61 ppm due to imine –N=C*H*, 8H triplet at δ 7.37 ppm, 16H quartet at δ7.15 ppm, 4H doublet at δ 7.00 ppm and 4H triplet at δ 6.93 ppm for aromatic protons. ^{13}C NMR spectrum showed two peaks at δ 162.3 and δ 161.2 ppm for carbons bearing -OH groups and carbons of schiff-base respectively, signal at δ 140.3 ppm for alkene carbons, whereas at δ (148.8, 133.2, 132.6, 132.3, 120.9, 119.2, 119.1, 117.3) ppm signals were observed due to aromatic carbons. The mass of compound **4** with HRMS technique was found to be 831.3654 which is in accordance to chemical formula of probe **4** ($C_{54}H_{40}N_4O_4Na^+$).

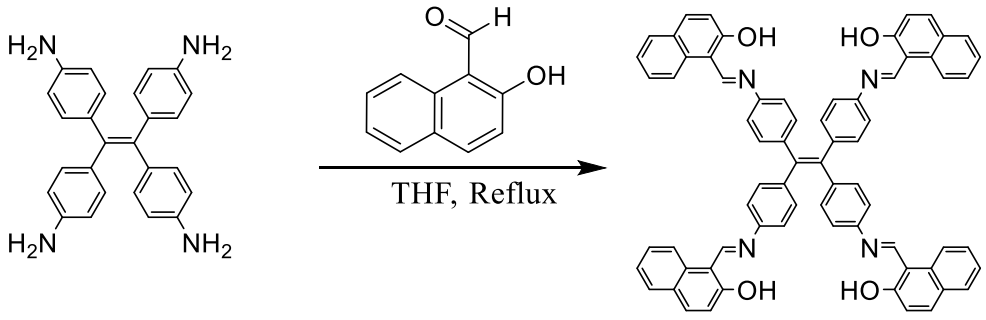

3 **5**

Scheme 3. Synthesis route for probe **5**

Synthesis of Probe 5. Probe **5** was synthesized by mixing the solution of compound **3** (0.02 g, 0.125 mmol) in THF with the solution of 2-hydroxynaphthaldehyde (0.08 g, 0.5 mmol) in THF. This mixture was refluxed for about 2 h and from the obtained mixture, THF was distilled off.

Bright orange colored compound **5** was obtained with 91.2% yield. ^{1}H NMR spectrum showed 4H singlet at δ 10.81 ppm for OH, 4H singlet δ 9.92 ppm for 4imine -N=C*H* protons and the peaks at δ (7.99, 7.78, 7.68, 7.63, 7.49 and 7.21) ppm were for protons of aromatic region. ^{13}C NMR spectrum showed two peaks at δ 162.7 and δ 162.8 ppm for carbons bearing -OH groups and carbons attached with nitrogen atoms by double bond respectively, at δ 140.31 ppm due to alkene carbons and rest of the peaks at δ (154.3, 142.3, 139.2, 131.2, 130.3, 128.9, 127.8, 125.1, 124.6, 123.3, 113.5) ppm were due to aromatic carbons. Also, the mass of compound **5** analyzed by HR-MS technique and was found to be 1031.3785 which is in accordance to chemical formula of probe **5** ($C_{70}H_{48}N_4O_4Na^+$).

4.2 Photophysical properties of Probe 4

4.2.1 Aggregation Induced Emission Enhancement (AIEE) Properties

The AIEE property of probe **4** was studied by using binary solvents; H_2O and THF. It was noticed in visible and long UV- light that on increasing water ratio in mixtures, the yellow color emitted by particles was intensified (**Figure 2**). Absorption and emission spectra at different water and THF ratios were recorded (**Figure 3**). Appreciable increase in intensity of absorption band in the mixtures of 70 to 90 percent water ratio was observed. The tailing off between 600-480 nm in absorption spectra showed the sign of aggregation. The fluorescence spectra at different water concentrations showed no effective change up to 70 percent water ratio mixtures but as the water ratio was increased further, the intensity of emission band noticeably increased and when water ratio increased to 90 percent the emission band boost up (**Figure 5**). So, collectively saying that when water content increased from 0 to 90 percent, emission band showed a red-shift of 22 nm with ~ 2-fold enhancement in emission intensity.

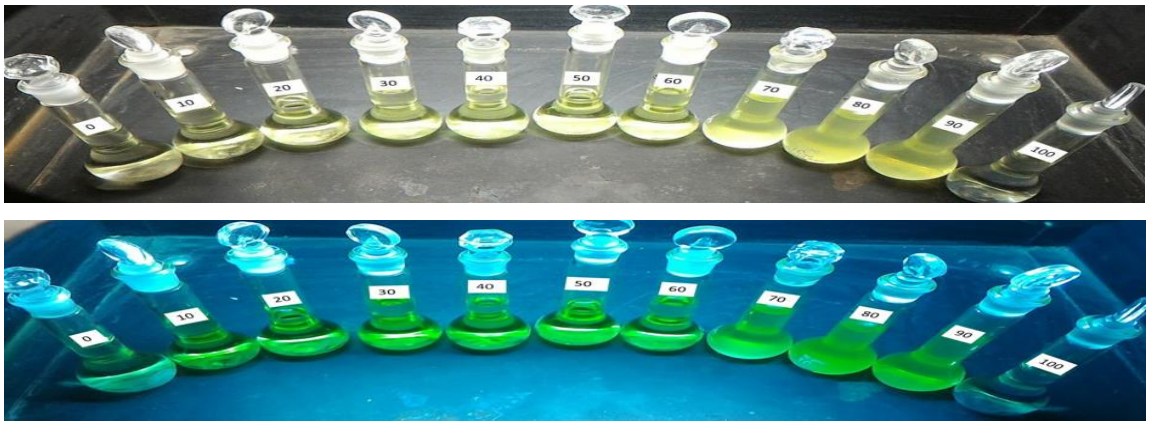

Figure 2: Emission intensity variation in day light and UV-light of 4 in binary solution (THF and Water) on increasing water fraction from left (0%) to right (100%).

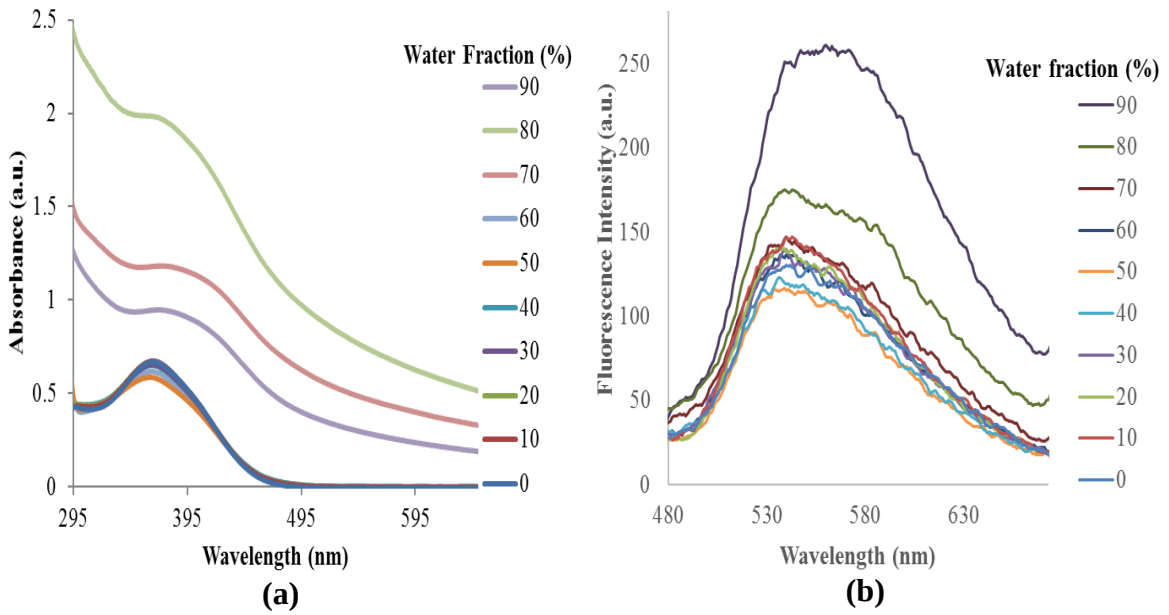

Figure 3: (a) UV-Visible spectra variation of probe 4 in THF, water and increasing water/THF ratio. **(ii)** Fluorescence spectra variation of probe 4 in THF, water and increasing water/THF ratio.

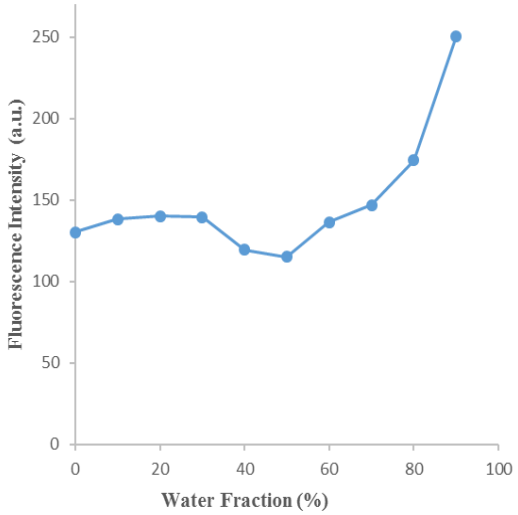

Figure 4: Plot of emission intensity (λ_{ex}= 360 nm, λ_{em}= 568 nm) (y-axis) vs increasing water fractions in THF (x-axis).

The aggregation of **4** was also supported by advance microscopic studies. FE-SEM images of probe **4** in THF and THF:H_2O (9:1) clearly depicted the aggregationproperties in the poor solvent. **Figure 5** showed that morphology was changed from spherically shaped dispersed particles (in pure THF) to needle shaped crystalline nano-aggregates THF:H_2O::9:1 mixture. The bathochromic shift of 22 nm in emission spectrum of probe **4** in THF:H_2O::9:1 could be explained due to morphological change from amorphous spheres to crystalline needle shaped aggregates.

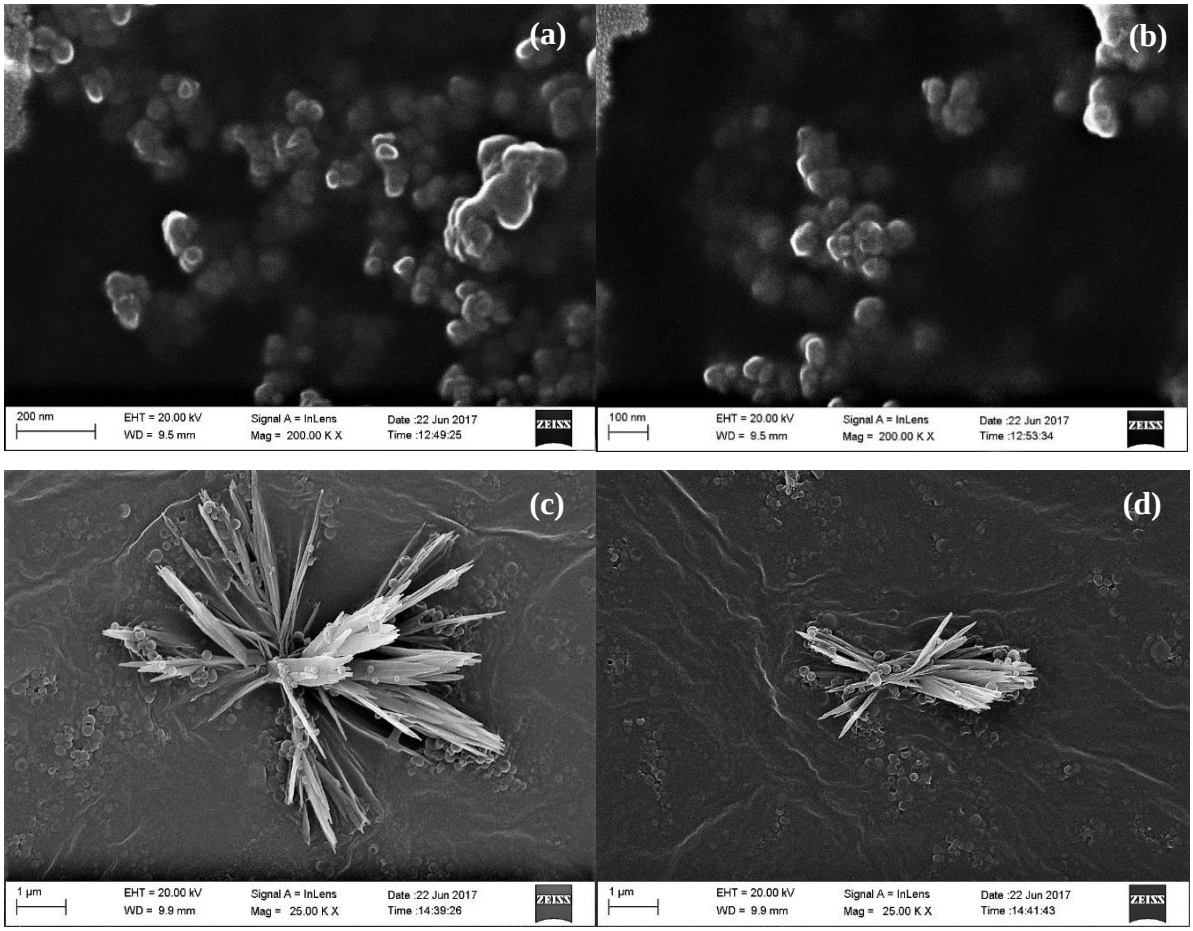

Figure 5: (a) and **(b)** FE-SEM images of probe **4** in pure THF. **(c)** and **(d)** FE-SEM images of probe **4** in 9:1 mixture of water and THF.

4.2.2 Chemosensing diagnosis of probe 4

In order to analyze the ion sensing ability of probe **4 (**20 µM, CH_3OH)was studied in presence and absence of various metal ions likeMg^{2+}, Al^{3+},K^{+}, Ca^{2+}, Fe^{2+}, Co^{2+},Ni^{2+}, Zn^{2+}, Ag^{+}, Hg^{2+}, etc.The probe **4** showed its absorption maxima at 368 nm. In the presence of various metal ions no significant change was observed except Al^{3+} ions (**Figure 6a)**.The presence of Al^{3+} ions to probe **4** showed a considerable quenching of absorption band at 378 nm. Upon incremental addition of Al^{3+} ions to probe **4** showed the concomitant decrease in absorption intensity and showed the linear behavior (**Figure 6b**). Upon excitation of probe **4** (20 µM, CH_3OH) at 378 nm showed the emission band at 547 nm. Large stokes shift of 169 nm was observed confirming the ESIPT phenomenon for probe **4**.

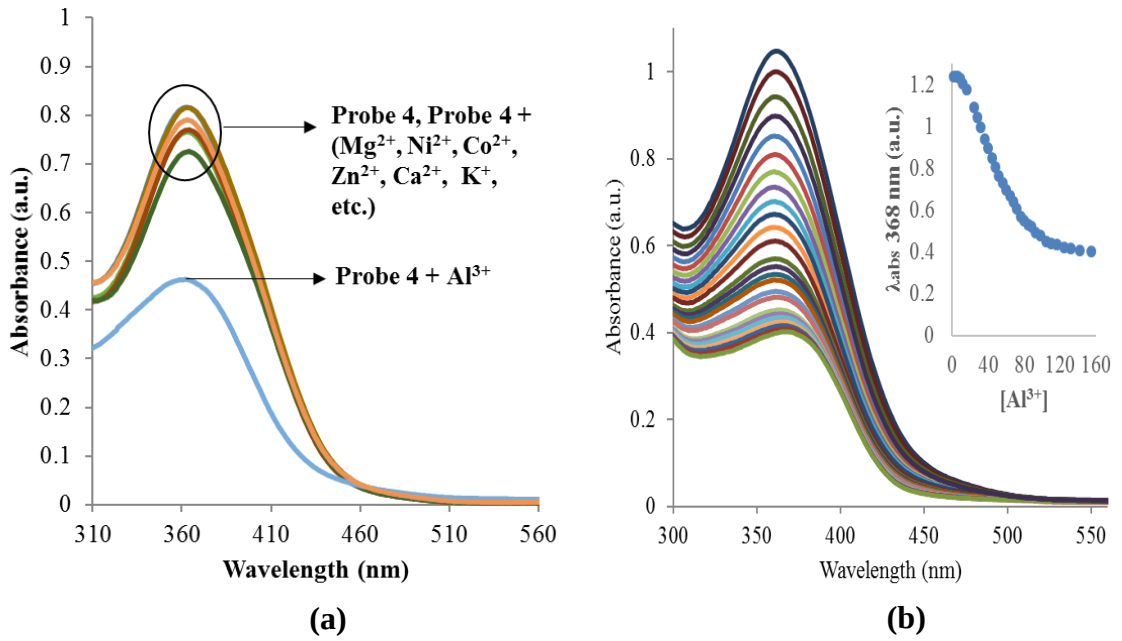

Figure 6: (a) UV-Visible spectra of probe **4** (20 µM, CH_3OH) in the presence of various metal ions; **(b)** Variation of UV-Visible spectra of Probe **4** (20 µM, CH_3OH) upon addition of Al^{3+} metal ions (0-154 µM); **(Inset)** Plot of absorbance intensity variation at 368 nm (y-axis) vs concentration of Al^{3+} metal ion (x-axis).

Upon addition of various metal ions like Mg^{2+},K^{+}, Ca^{2+}, Fe^{2+}, Co^{2+},Ni^{2+}, Zn^{2+}, Ag^{+}, Hg^{2+}, etc., no observable change was observed in the presence of metal ions except in the presence of Al^{3+} ion. The presence of Al^{3+} ions to solution of probe **4** decolorizes the solution when observed in visible light and showed the green fluorescent color in the UV light (**Figure 7).** Upon successive addition of $Al^{3+}$to the solution of probe **4**(20µM, CH_3OH) resulted in blue shift of emission band from 547 to 467 nm with 7.5-fold emission enhancement (**Figure 8**). Thus, probe **4** was referred as naked-eye turn-on fluorescent chemosensor for Al^{3+} ions. The probe 4 showed good stability constant of 1.8×10^{4} $mol^{-1}$and appreciable detection limit of 0.47 µM Al^{3+} ions.

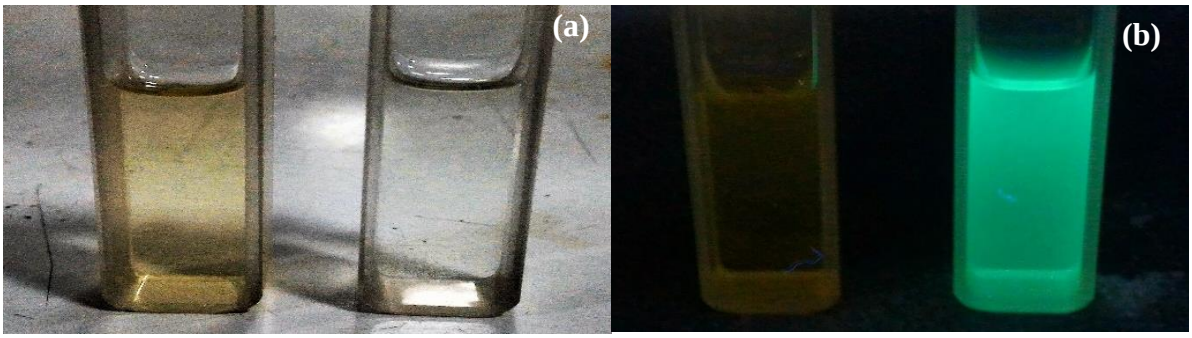

Figure 7: (a) Color change in visible light. **(b)** Emission change in UV-light

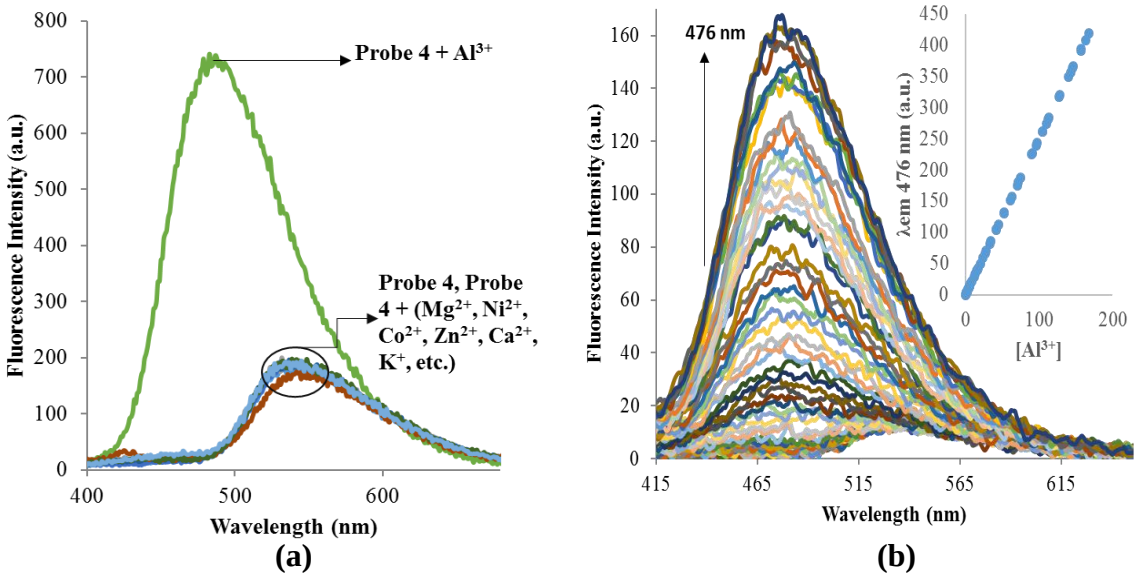

Figure 8: (a) Effect of various metal ions on emission spectra of Probe **4; (b)** Fluorescence spectra (λ_{ex}=368nm) variation of Probe **4** (2.5 µM) upon addition of Al^{3+} (0 - 21.25 µM)in methanol. **(Inset)** Plot of fluorescence intensity of probe **4** (2.5µM) variation at 477 nm (y-axis) and addition of Al^{3+} ion concentration (x-axis).

The emission studies of probe **4** in the presence of Al^{3+} ion showed the drastic emission enhancement. The results depicted the Al^{3+} ion induced emission enhancement probably due to formation of aggregates. In order to study the ion induced aggregation properties FE-SEM images were recorded in the presence and absence of Al^{3+} ions. FE-SEM images in the presence of Al^{3+} ions showed the morphological changes from spheres to triangular shape. Probe **4** (20 µM, CH_3OH) solution showed buds like morphology whereas on doping with Al^{3+} ions, shape of molecules turned to triangular flakes **(Figure 9)**.

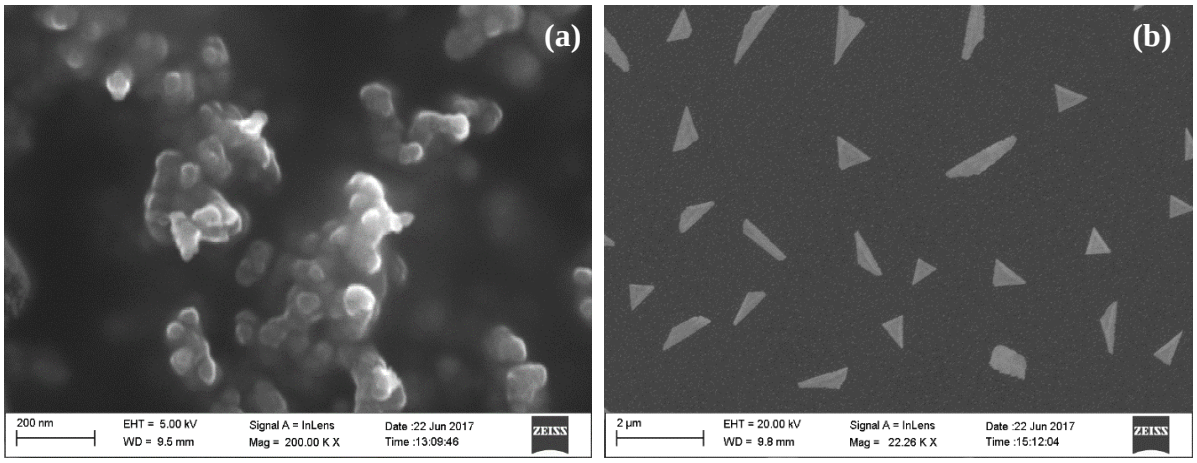

Figure 9: (a) FE-SEM images of probe **4** and **(b)** Probe **4** + Al^{3+} metal ions in methanol solution.

4.2.3 Practical applicability

In order to discover the practical applicability of probe **4**, competitive cation experiment was performed. Solution of probe **4** (2.5μM, CH_3OH) in the presence of 1000 μM of Al^{3+} metal ions in methanol, 1000 μM of each cation (Mg^{2+}, Al^{3+}, K^{+}, Ca^{2+}, Fe^{2+}, Ni^{2+}, Zn^{2+}, Ag^{+}, Hg^{2+}, Co^{2+}, etc.) was added and their emission spectra were recorded. **Figure 10** clearly depicted that presence of other metal ions did not infer the changes attained in the presence of Al^{3+} ions at 476nm. These analysis ensures that probe **4** is highly selective towards Al^{3+} ions.

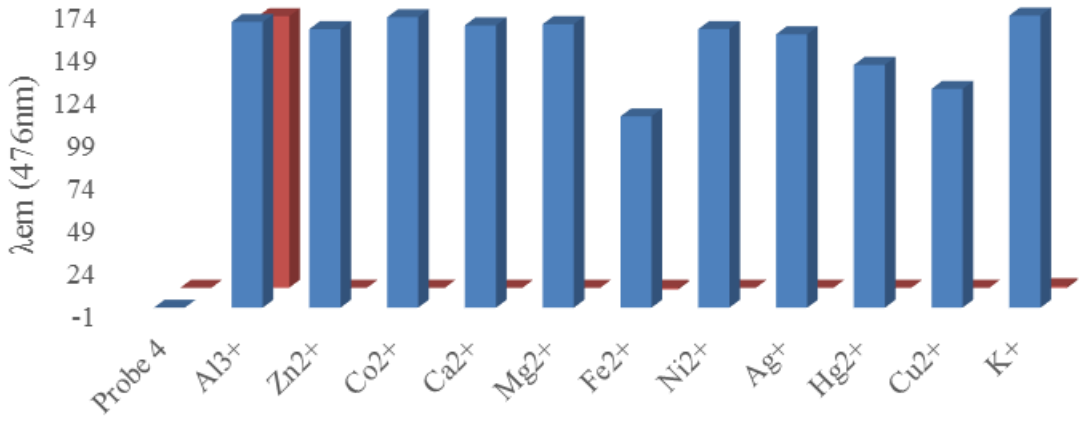

Figure 10: Red bars show selectivity of probe **4** (2.5 μM) (λ_{ex}=368 nm, slit width = 10) upon addition of different cations (1000 μM) in methanol and Blue bars show the competitive selectivity of **4** in the presence of Al^{3+}metal ions.

4.3 Photophysical properties of Probe 5

4.3.1 Aggregation Induced Emission Enhancement (AIEE) Properties

Aggregation induced emission enhancement properties of probe **5** studied in binary mixture of THF and poor solvent H_2O. Probe **5** (10 μM) solution was mixed in different ratios of water.Absorption spectra of probe **5** (10 μM, THF)showed the absorption maxima at 409 nm. Upon incremental addition of H_2O upto 1:1 showed the red shift of 49 nm and upon further increasing the H_2O ratio caused the decrease in absorption intensity (**Figure 10 (a)**). Emission spectra of probe **5** (10 μM, THF) showed emission maxima at 541 nm (**Figure 10 (b)**). Upon incremental addition of H_2O upto 1:1 showed the red shift of 15 nm and upon further increasing the H_2O ratio caused the decrease in emission intensity along with red shift of 28 nm.The observed red shift was associated with the emission color change from light green to red under UV-light as shown in **Figure 11**.

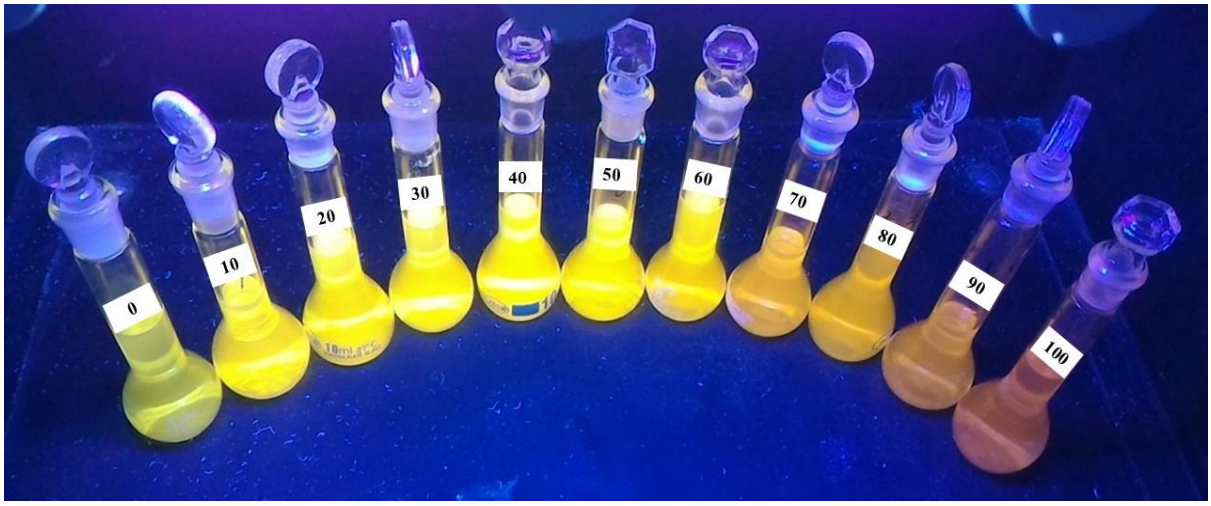

Figure 11: Emission intensity variation and color shift in UV-light of probe **5**in binary solution (THF and Water) on increasing water fraction from left (0%) to right (100%).

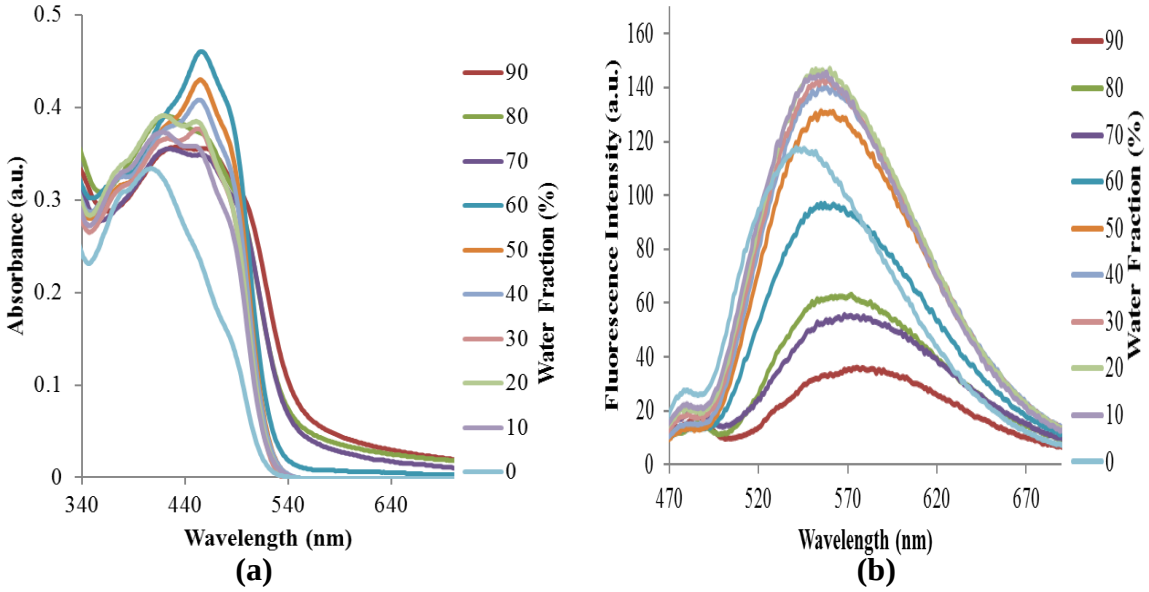

Figure 12: (a) UV-Visible and **(b)**Fluorescence spectra variation of probe **5(10**µM) in THF, water and increasing water/THF ratio.

The aggregation of probe **5** was supported by advance microscopic studies; i.e. FE-SEM. FE-SEM images gave a clear picture of aggregation due to their morphological changefrom spherically shaped dispersed particles (in THF) to randomly agglomerated cluster [in H_2O: THF (9:1) mixture] **Figure 15.**

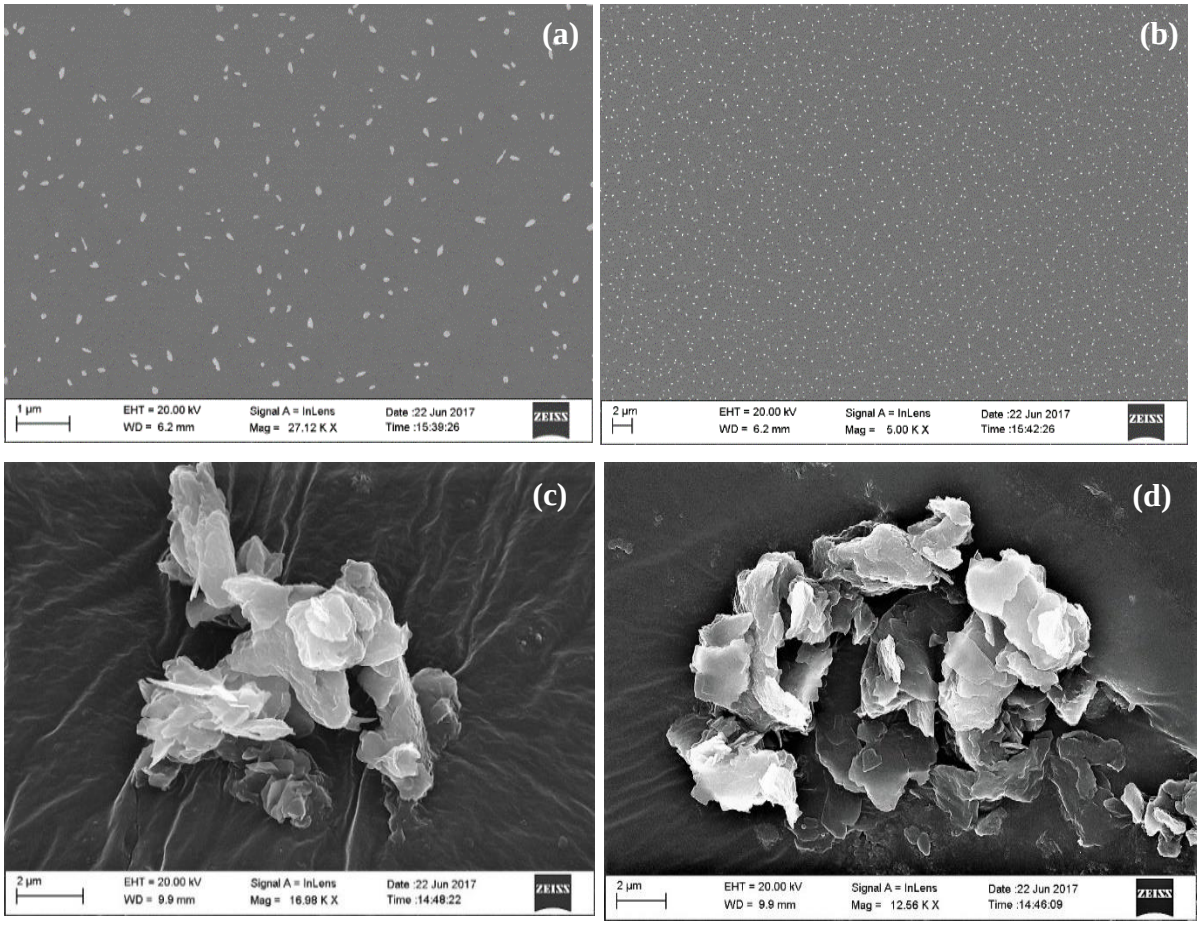

Figure 13: (a) and **(b)** FE-SEM images of probe **5** in pure THF. **(c)** and **(d)** FE-SEM images of probe **5** in 9:1 mixture of water and THF.

4.3.2 Chemosensing diagnosis of Probe 5

Now, to determine sensing characteristic qualitatively of probe **5**, a similar kind of studies was performed as in case of probe **4**. Absorption spectra of probe **5** were recorded in presence and absence of various metal ions like Mg^{2+}, Al^{3+}, K^{+}, Ca^{2+}, Fe^{2+}, Co^{2+}, Ni^{2+}, Zn^{2+}, Ag^{+}, Hg^{2+}, etc. Probe **5** showed it`s absorption maxima at 460 nm. In the presence of various ions, no appreciable change was observed except Al^{3+} ions (**Figure 14 a**).The presence of Al^{3+} ions showed 2.5-fold quenching at 460 nm and gradual enhancement of bands at 400 nm and 310 nm (**Figure 14 b**). Upon excitation of probe **5** (20 µM, CH_3CN) at 402 nm showed the emission band at 562 nm. Large stokes shift of 160 nm was observed confirming the ESIPT phenomenon for probe **4**.The presence of Al^{3+} ions to solution of probe **5**fades the color of solution as observed in visible light (**Figure 15).**

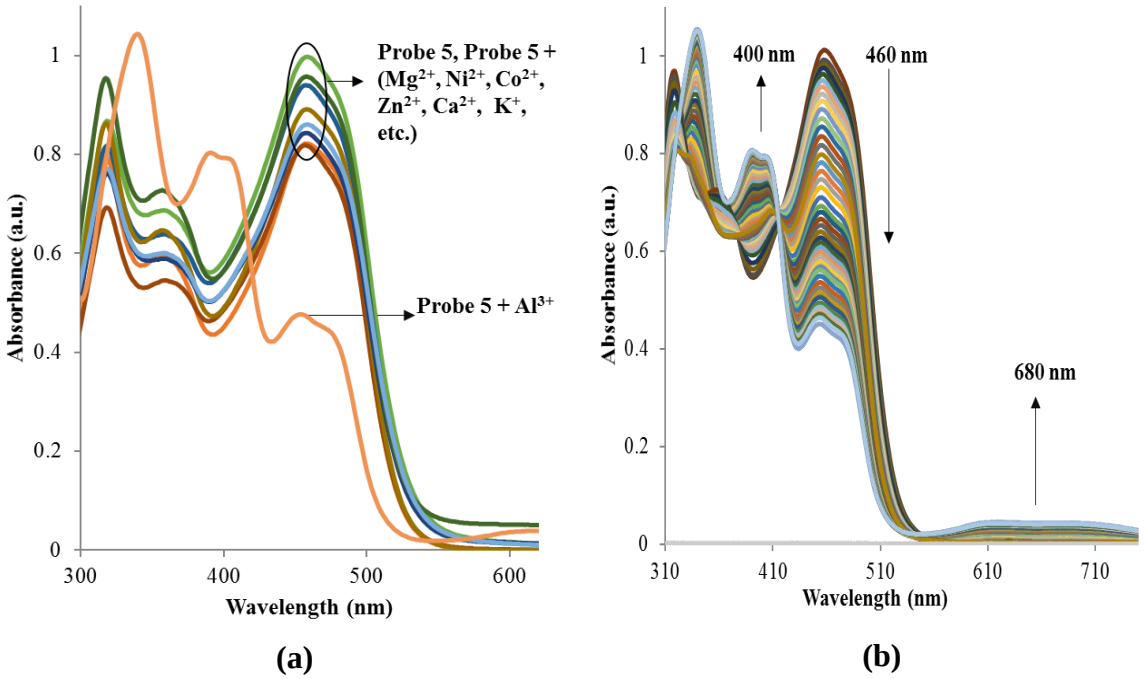

Figure 14: (a) Absorption spectra of probe **5** (20 µM, CH_3OH) in the presence of various metal ions; **(b)** Variation in UV-Visible spectra of Probe **5** (20 µM, CH_3OH) upon addition of Al^{3+} metal ions (0-80 µM).

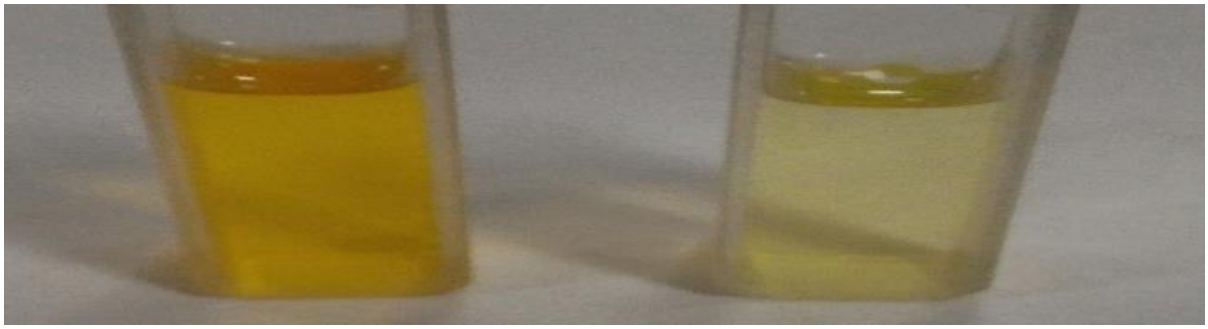

Figure 15: Naked-eye visible color change of probe **4** in the presence of Al^{3+}.

Probe **5** solution (20 µM, CH_3OH) showed it`s emission band at 570 nm upon excitation at 460 nm. On treatment of **5** (20 µM, CH_3OH) with various cations like Mg^{2+},K^+, Ca^{2+}, Fe^{2+},Co^{2+}, Ni^{2+}, Zn^{2+}, Ag^+, Hg^{2+}, etc., no observable change was observed in the presence of metal ions except in the presence of Al^{3+} ion (**Figure 16 a**). Upon successive addition of 0.4 equivalents of Al^{3+}ions to the solution of probe **5**(20 µM, CH_3OH) resulted inincrease in intensity of band with a blue shift of 12 nm (**Figure 16 b**) and then on further addition of metal ion (up to 2.35 equivalents) lead to decrease in intensity of band along with slight blue shift of 8 nm (**Figure 16 c**). Thus, probe **5** was referred as naked-eye turn-on fluorescent chemosensorfor Al^{3+} ions. The probe **5** showed good stability constant of 5.6×10^4 $mol^{-1}$and effectivedetection limit of 0.3 µM Al^{3+} ions.

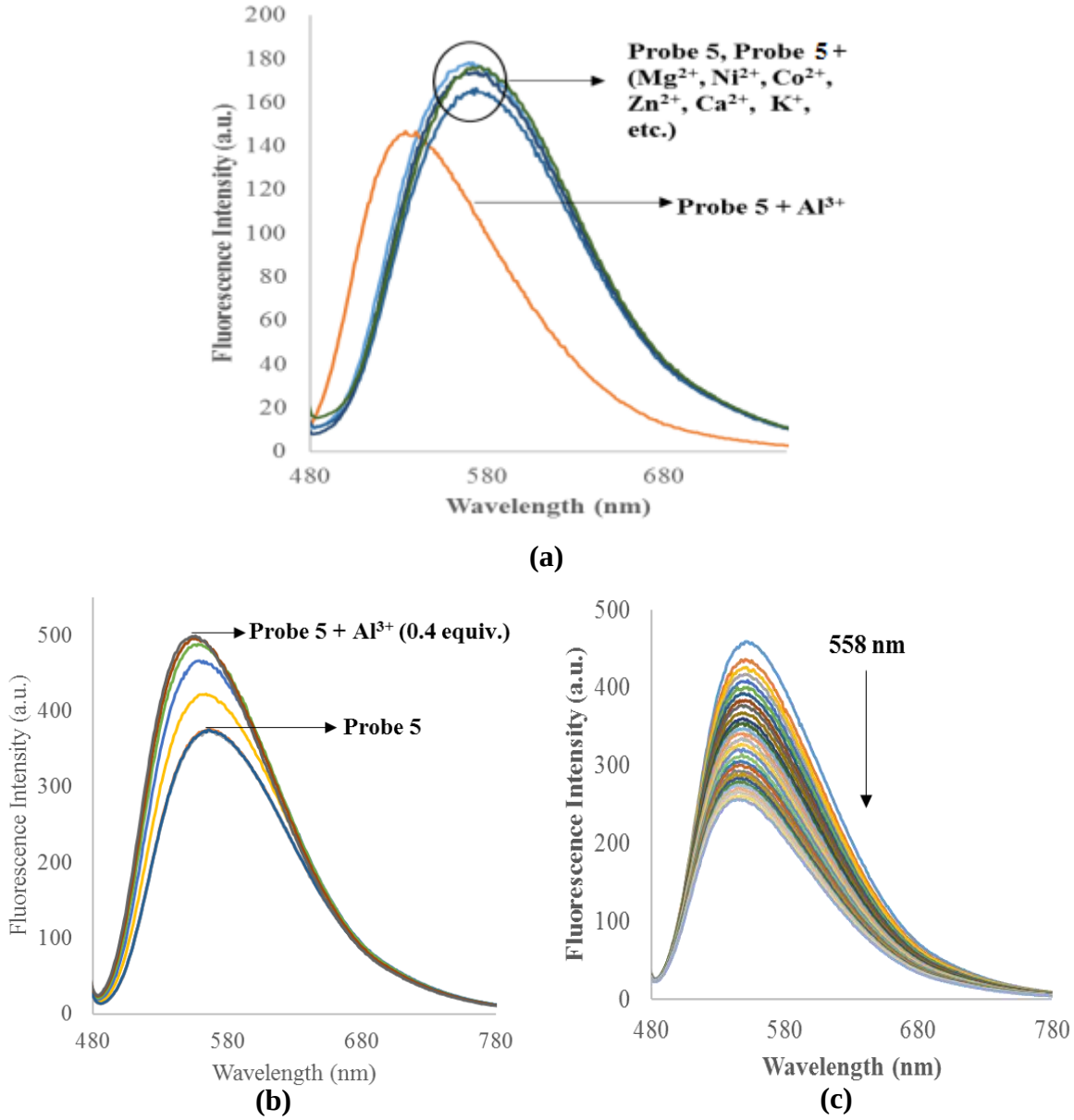

Figure 16: (a) Emission spectra of probe **5** (20µM, CH_3OH) in the presence of various metal ions; **(b)** Effect of incremental addition of Al^{3+} ions between 0-0.4 equiv. to probe **5** (20µM, CH_3OH, λ_{ex}=460nm); **(c)** Effect of incremental addition of Al^{3+} ions between 0.6 – 2.35 equiv. to probe **5** (20µM, CH_3OH, λ_{ex}=460nm).

From the FE-SEM studies, it was clearly depicted that this sensing is the result of aggregation of the molecules of probe **5 (Figure 17)** in the presence Al^{3+} ions.Probe **5**(20 µM, CH_3OH) solution showed spherically dispersed particles and on doping Al^{3+} metal ions to the same solution these particles aggregate.

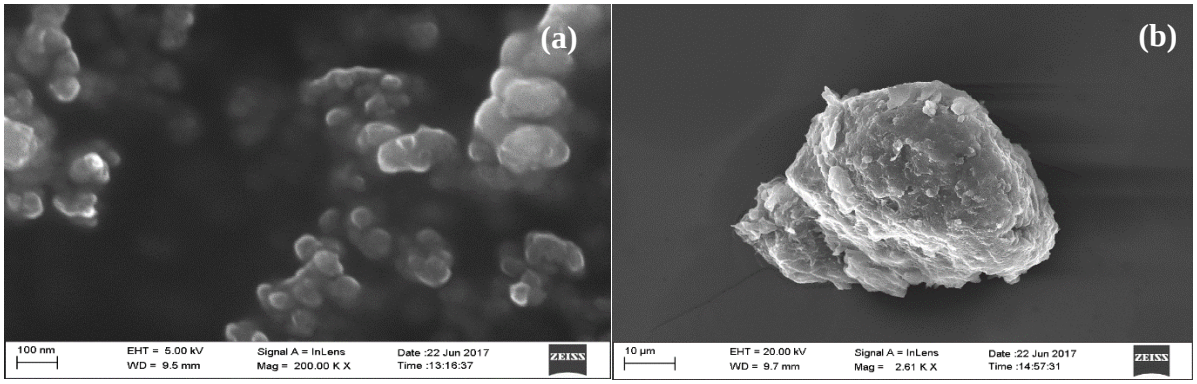

Figure 17: (a) FE-SEM images of probe **5**(20 µM, CH_3OH) and **(b)** Probe **5**(20 µM, CH_3OH) + Al^{3+} ions.

4.3.3 Practical applicability

In order to discover the practical applicability of probe **5**, competitive cation experiment was performed. 20 µM solution of probe **5** (20 µM, CH_3OH) was doped with 1000 µM of Al^{3+}metal ions and 1000 equiv. of each competitive cation (K^+, Ca^{2+}, Mg^{2+}, Fe^{2+}, Ni^{2+}, H^+, Zn^{2+}, Ag^{2+}, Hg^{2+}, Co^{2+}, etc.) was added and their absorption spectra were recorded. **Figure 18** clearly showed that the presence of any cation did not modify the changes recorded in the presence of Al^{3+} ions at 460 nm. This ensures that probe **5** is quite selective towards Al^{3+} ions.

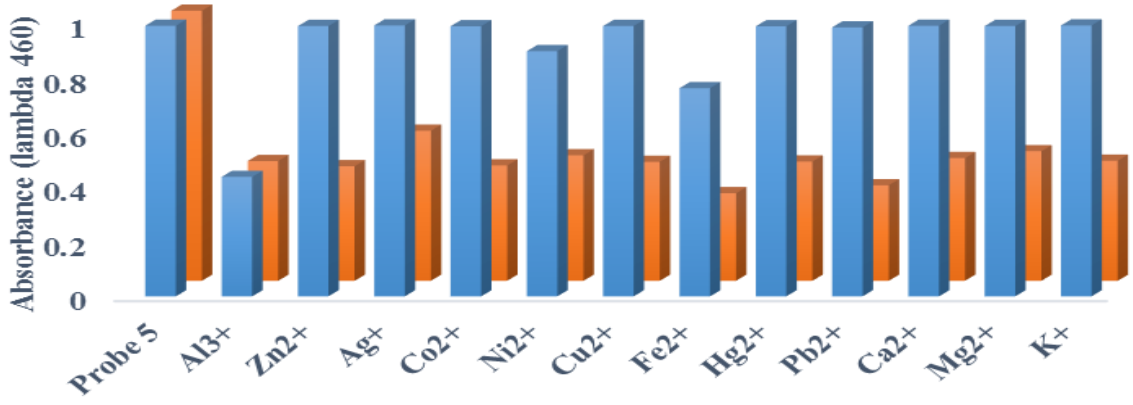

Figure 18: Blue bars show selectivity of probe **5** (20 µM) upon addition of different cations (1000µM) in methanol and orange bars show the competitive selectivity of **5** in the presence of Al^{3+} ions.

Chapter-5
Conclusion and Future Scope

5.1 Conclusion

We have successfully synthesized TPE-based Schiff bases **4** and **5** with four receptor sites onto single fluorogenic platform. The TPE-fluorogens showed AIEE phenomenon in the poor solvents and showed the light up fluorogen behavior. AIEE-characteristic of probes **4** and **5** has been used for sensing of Al^{3+} ions. The detection of Al^{3+} ion was based on ion-induced aggregation phenomenon. The AIEE-feature and ion-induced aggregation phenomenon of **4** and **5** has been proved by UV-Visible, Fluorescence and FE-SEM studies. The probes **4** and **5** showed the lowest detection limit of 0.47 μM and 0.3 μM respectively. The probe **4** upon aggregation showed morphological change from amorphous spheres to crystalline needles whereas probe **5** showed morphological change from spheres to agglomerated clusters.

5.2 Future Scope

The combination of AIEE and ESIPT properties of probe **4** and **5** can be effectively used in OLEDs, mechanochromophores and in other optical chemo-sensors. From the results of present compounds, new probes could be synthesized to fine tune the desired properties of sensors, OLEDs, mechanochromophores by incorporating other sensing phenomenons like TICT, RIR, ICT etc.

Bibliography

1 L. E. Santos-Figueroa, M. E. Moragues, E. Climent, A. Agostini, R. Martínez-Máñez and F. Sancenón, *Chem. Soc. Rev.*, 2013, **42**, 3489.

2 S. Zhang and T. M. Swager, 2003, *J. Am. Chem. Soc.*, 2003, **125**, 3420–3421.

3 J. Wu, W. Liu, J. Ge, H. Zhang and P. Wang, *Chem. Soc. Rev.*, 2011, **40**, 3483–3495.

4 T. Terai and T. Nagano, *Curr. Opin. Chem. Biol.*, 2008, **12**, 515–521.

5 J. H. Ye, J. Liu, Z. Wang, Y. Bai, W. Zhang and W. He, *Tetrahedron Lett.*, 2014, **55**, 3688–3692.

6 C. Wang, Y. Liu, J. Cheng, J. Song, Y. Zhao and Y. Ye, *J. Lumin.*, 2015, **157**, 143–148.

7 C. Y. Li, Y. Zhou, Y. F. Li, C. X. Zou and X. F. Kong, *Sensors Actuators, B Chem.*, 2013, **186**, 360–366.

8 T. Gunnlaugsson, H. D. P. Ali, M. Glynn, P. E. Kruger, G. M. Hussey, F. M. Pfeffer, C. M. G. Dos Santos and J. Tierney, *J. Fluoresc.*, 2005, **15**, 287–299.

9 J. Zhao, S. Ji, Y. Chen, H. Guo and P. Yang, *Phys. Chem. Chem. Phys.*, 2012, **14**, 8803–17.

10 X. Qi, E. J. Jun, L. Xu, S. Kim, J. Sung, J. Hong, Y. J. Yoon and J. Yoon, Chem. Soc. Rev., 2006, **210**, 2881–2884.

11 V. S. Padalkar and S. Seki, *Chem. Soc. Rev.*, 2016, **45**, 169–202.

12 J. Huang, N. Sun, J. Wang, R. Tang, X. Li, J. Dong, Q. Li, D. Ma and Z. Li, *Isr. J. Chem.*, 2014, **54**, 931–934.

13 J. Li, Y. Jiang, J. Cheng, Y. Zhang, H. Su, J. W. Y. Lam, H. H. Y. Sung, K. S. Wong, H. S. Kwok and B. Zhong Tang, *Phys. Chem.*, 2011, **17**, 1134–1141.

14 D. Ding, K. Li, B. Liu and B. Z. Tang, *Acc. Chem. Res.*, 2013, **46**, 2441–2453.

15 Y. Liu, C. Deng, L. Tang, A. Qin, R. Hu, J. Z. Sun and B. Z. Tang, *J. Am. Chem. Soc.*, 2011, **133**, 660–663.

16 J. Liang, B. Z. Tang and B. Liu, *Chem. Soc. Rev.*, 2015, **44**, 2798–811.

17 H. Tong, Y. Hong, Y. Dong, M. Haeussler, J. W. Y. Lam, Z. Li, Z. Guo, Z. Guo and B. Z. Tang, *Chem. Commun.*, 2006, **311**, 3705–3707.

18 L. Liu, G. Zhang, J. Xiang, D. Zhang and D. Zhu, *Org. Lett.*, 2008, **10**, 4581–4584.

19 Q. Chen, N. Bian, C. Cao, X.-L. Qiu, A.-D. Qi and B.-H. Han, *Chem. Commun. (Camb).*, 2010, **46**, 4067–4069.

20 C. Park and J. I. Hong, *Tetrahedron Lett.*, 2010, **51**, 1960–1962.

21 Y. Hong, S. Chen, C. W. T. Leung, J. W. Y. Lam, J. Liu, N. W. Tseng, R. T. K. Kwok, Y. Yu, Z. Wang and B. Z. Tang, *ACS Appl. Mater. Interfaces*, 2011, **3**, 3411–3418.

22 F. Sun, G. Zhang, D. Zhang, L. Xue and H. Jiang, *Org. Lett.*, 2011, **13**, 6378–6381.

23 J. H. Ye, L. Duan, C. Yan, W. Zhang and W. He, *Tetrahedron Lett.*, 2012, **53**, 593–596.

24 J. H. Ye, L. J. Duan and L. L. Jin, *Adv. Mater. Res.*, 2012, **554**–**556**, 2045–2048.

25 D. Zhang, X. Huang, X. Gu and G. Zhang, *Chem. Commun.*, 2012, **81**, 12195–12197.

26 Y. Yan, Z. Che, X. Yu, X. Zhi, J. Wang and H. Xu, *Bioorganic Med. Chem.*, 2013, **21**, 508–513.

27 H. T. Feng, X. Zhang and Y. S. Zheng, *J. Org. Chem.*, 2013, **80**, 8096–8101.

28 X. Gu, G. Zhang, Z. Wang, W. Liu, L. Xiao and D. Zhang, *Analyst*, 2013, **138**, 242724–31.

29 I. Simsek Turan, F. Pir Cakmak and F. Sozmen, *Tetrahedron Lett.*, 2014, **55**, 456–459.

30 H. T. Feng and Y. S. Zheng, *Chem. - A Eur. J.*, 2014, **20**, 195–201.

31 S. Gui, Y. Huang, F. Hu, Y. Jin, G. Zhang, L. Yan, D. Zhang and R. Zhao, *Anal. Chem.*, 2015, **87**, 1470–4.

32 D. G. Khandare, H. Joshi, M. Banerjee, M. S. Majik and A. Chatterjee, *Anal. Chem.*, 2015, **87**, 10871–10877.

33 V. Mahendran, K. Pasumpon, S. Thimmarayaperumal, P. Thilagar and S. Shanmugam, *J. Org. Chem.*, 2016, **81**, 3597–3602.

34 A. Sen Gupta, K. Paul and V. Luxami, *Sensors Actuators B Chem.*, 2017, **246**, 653–661.

Pranshu_06-07-2017

ORIGINALITY REPORT

%7	%4	%5	%3
SIMILARITY INDEX	INTERNET SOURCES	PUBLICATIONS	STUDENT PAPERS

PRIMARY SOURCES

1	Ji Eon Kwon. "Advanced Organic Optoelectronic Materials: Harnessing Excited-State Intramolecular Proton Transfer (ESIPT) Process", Advanced Materials, 08/23/2011 Publication	%1
2	Sarkar, Deblina, Ajoy Kumar Pramanik, and Tapan Kumar Mondal. "Benzimidazole based ratiometric and colourimetric chemosensor for Ni(II)", Spectrochimica Acta Part A Molecular and Biomolecular Spectroscopy, 2016. Publication	%1
3	www.google.nl Internet Source	<%1
4	Lee, S.. "High temperature synthesis of silicalite-1 in cationic microemulsions", Microporous and Mesoporous Materials, 20051128 Publication	<%1
5	dspace-unipr.cineca.it Internet Source	<%1